UILU-ENG 85-3604

Report No. 120

SERVICE LOAD HISTORIES ANALYZED BY THE LOCAL STRAIN APPROACH

by

Thomas F. Fugger, Jr.
Department of Theoretical and Applied Mechanics

A Report of the

MATERIALS ENGINEERING - MECHANICAL BEHAVIOR

College of Engineering, University of Illinois at Urbana-Champaign

May 1985

ABSTRACT

Design of ground vehicle components has become increasingly dependent on the ability to predict the service fatigue life accurately. The local strain approach is one fatigue design method which has been employed to predict fatigue life of a component subject to service conditions.

Evaluation of the accuracy of the local strain approach and the influence of mean stresses was achieved in the present study by analyzing the behavior of smooth specimens subjected to three service strain histories. These histories were used to obtain the corresponding block stress history and number of blocks to failure. Stress response was analytically predicted to allow comparison to the actual recorded stress response. Predicted and actual mean stresses were incorporated into the analysis to investigate the sensitivity of the local strain approach to mean stresses.

Mean stresses determined from the predicted stress response were found to be nonconservative with regard to the damage calculation when compared to the actual stress response. Predicted fatigue lives incorporating either measured or predicted mean stresses were found to be within a factor of two of the experimental data. Lives obtained by ignoring mean stresses were up to a factor of three higher in comparison to the mean stress correction values.

ACKNOWLEDGMENTS

This research was conducted in the Materials Engineering Research Laboratory located in Talbot Laboratory, University of Illinois at Urbana-Champaign. Funding was provided through a gift from the Firestone Tire and Rubber Company - Central Research Laboratories to the Department of Theoretical and Applied Mechanics.

The author would like to thank Dr. Peter Kurath and Mr. Daniel Morrow of the Mechanical and Industrial Engineering Department at the University of Illinois for their patience and technical support during the progress of this research. Further assistance was provided by Messrs. David Stalnaker and Arthur Dory of the Firestone Tire and Rubber Company. The assistance provided to the author by Professors JoDean Morrow and Herbert T. Corten is appreciated. The John Deere Company, Moline, Illinois, is gratefully acknowledged for performing the chemical analysis of the test material. Further thanks are extended to Darlene Mathine for her patience in preparing the manuscript.

TABLE OF CONTENTS

LIST OF TABLES

LIST OF FIGURES

LIST OF SYMBOLS

b	Fatigue strength exponent
B_f	Number of blocks to failure
c	Fatigue ductility exponent
D	Fatigue damage
D_B	Fatigue damage for one block of the applied history
D_i	Fatigue damage for cycle i
E	Elastic modulus (ksi)
k	Number of events identified by rainflow counting
K	Strength coefficient (ksi)
K'	Cyclic strength coefficient (ksi)
n	Strain hardening exponent
n'	Cyclic strain hardening exponent
N	Number of applied cycles
N_f	Number of cycles to failure
N_i	Number of repetitions of cycle i
$(N_f)_i$	Number of cycles to failure for cycle i
$\Delta\varepsilon/2$	Strain amplitude
$\Delta\varepsilon_e$	Elastic strain range
$\Delta\bar{\varepsilon}_e/2$	Half life elastic strain amplitude
$\Delta\varepsilon_p$	Plastic strain range
$\Delta\bar{\varepsilon}_p/2$	Half life plastic strain amplitude
$\Delta\varepsilon_t$	Total strain range
$\Delta\bar{\sigma}/2$	Half life stress amplitude
ε	Strain
ε_f'	Fatigue ductility coefficient

σ	Stress (ksi)
σ_a	Stress amplitude (ksi)
σ_o	Mean stress (ksi)
σ_y	.2% offset yield strength (ksi)
σ'_f	Fatigue strength coefficient (ksi)

1. INTRODUCTION

1.1 Background

Low cost, structural grade steels are found in many components used by the ground vehicle industry. Techniques for estimating the fatigue lives of these components subjected to complex service histories have long been of primary concern to the industry [1].[1]

One technique for estimating fatigue lives of components uses the local strain approach. This method employs a typical service load history, the material properties, and the component geometry to obtain the cyclic strain response at a critical location (Fig. 1). Local stress and strain excursions are separated into damaging events which are then summed to estimate service fatigue life. A flowchart depicting this procedure appears in Fig. 2. This method has been refined over several decades by researchers from several industrial backgrounds [3-7].

Two considerations implemented in the local strain approach are the event identification and damage summation techniques. Several methods available for identifying damaging events [8] include range pairing, level crossing, and rainflow counting. These methods reduce a complex loading history to a series of events to which damage values can be assigned employing the material's fatigue properties. A summation technique is then used to predict failure. Linear damage accumulation for each identified event, known as the Palmgren-Miner hypothesis [9], is the simplest damage summation technique.

---

[1]Numbers in brackets indicate reference at the end of the report.

1.2 Scope

This research incorporates the concepts of the local strain approach to obtain service fatigue life estimates for a non-specific ground vehicle component. Estimation of the fatigue life is accomplished by analyzing data obtained at three critical regions on the component.

Smooth specimens are subjected to sequential peak-valley service strain histories to obtain the corresponding block stress history and the number of blocks to failure. The block stress history is analytically predicted using an availability matrix concept. Analysis of the strain history by the local strain approach allows comparison of the actual stress response and the predicted stress response. The effect of mean stress on component service life is determined by including mean stresses in the damage calculation. Due to limited testing time, service strain histories have been amplified by a scale factor. Mean stress effects are considered in the life prediction analysis for the scaled histories, though the plasticity introduced by amplification has reduced their effect. Lower scale factor service histories are analyzed and mean stress effects are discussed.

2. COMPONENT SPECIFICATIONS

2.1 Geometry

Locations on the component for data collection of service histories are selected based upon a review of service failures. Three locations are found to develop cracks. These locations will be referred to as location A, B and C. Since strain gages are placed at the "critical" locations on the component, no assumption with regard to the corresponding nominal loading and local strain behavior will be necessary. This eliminates one assumption and possible inaccuracy in the local strain analysis.

2.2 Loading History

The loading history is separated into two categories: (1) offset strain and (2) service strains. Offset strains are those which the component experiences during fabrication prior to service load application. The value of this strain is noted before the service history is recorded. It is known that this value does not remain constant during the life of the component. However, a constant value has been assumed for the ensuing analysis.

The service strain history for this investigation was recorded on FM tape during several laps on a test track facility by the sponsor of this research. Sixteen-minute segments for each location on the component have been selected by the sponsor of this research as representative of the complete loading history. Digitization of the analog signal was to 12-bit precision corresponding to a full scale value of 1000 microstrain. The three histories investigated are shown, without the offset strains, in Figs. 3-5 and are subsequently referred to as histories A, B and C. Values obtained for the offset strain are +0.001, 0, and -0.0004 for history A, B and C, respectively.

3. BASELINE MATERIAL CHARACTERIZATION

3.1 Material

Two fully annealed 1015 steel plates of 3/8-inch thickness were provided by the Firestone Tire and Rubber Company - Central Research Laboratories. A chemical analysis is shown in Table 1. A cross-section of the material's microstructure indicates the coarse grained pearlitic structure common to annealed steels (Fig. 6).

3.2 Specimen Design

A flat plate specimen with an unpolished surface as received from the manufacturer and a polished round specimen (Fig. 7) are employed to evaluate the effects of the surface condition on the material's fatigue behavior. These effects were found to be negligible, and the round specimen was used for the remainder of the project. Specimens are machined with their longitudinal axes normal to the rolling direction of the plates corresponding to the anticipated weakest direction.

3.3 Monotonic and Cyclic Material Properties

Monotonic tensile tests are performed to determine the stress-strain properties for annealed 1015 steel [11]. These results are presented in Table 2.

Completely reversed, constant amplitude, strain controlled tests were performed to determine the baseline fatigue properties [12,13]. Specimen separation was the definition of failure for this investigation. Data obtained from the strain-life tests are summarized in Table 3. The strain-life curve determined from these data is given in Fig. 8.

These data are then used to determine a cyclic stress-strain curve by fitting a Ramberg-Osgood relation [12]:

$$\varepsilon = \frac{\sigma}{E} + \left(\frac{\sigma}{K'}\right)^{1/n'} \qquad (1)$$

where coefficients K' and n' are determined from the values of stress and plastic strain amplitude obtained at the half life of the fatigue tests (Table 3). A graphical representation of the results and the corresponding coefficients are given in Fig. 9. The cyclic stress-strain curve obtained from these coefficients is displayed in Fig. 10. Values for the strain life and cyclic stress-strain constants are presented in Table 4.

4. ANALYSIS TECHNIQUE

4.1 Mean Stress Effects

Mean stresses may significantly affect the fatigue life for a given strain range [15]. If inelastic deformation occurs, the corresponding stress-time response will vary greatly depending on the sequence of events, as illustrated by the stress-strain response shown in Fig. 11. The excursion from point A to point D results in a considerable amount of plastic flow. As a result, events B-C-B and F-G-F, which are of equal strain excursion, have significantly different stress responses. Identification of the correct stress excursion becomes important if mean stresses affect the damage calculations.

Differences in service life estimates due to separation of the loading history into two categories for this investigation (offset strain and service strain) are of interest here. Offset strains will influence the initial stress-strain level and mean stresses for the subsequent service strain history. Observation of the offset strain effect on the service life estimates provides some indication of the importance of these initial strain excursions. Mean stress relaxation, which may alter the initial mean stress level, is not considered in this report.

To evaluate the influence of mean stresses, one can compare the service life predictions obtained without accounting for mean stresses with the predicted lives computed which include these levels. The mean stress levels are determined by two methods: (1) analysis of the actual stress response of a specimen subject to the strain history; and (2) computer simulation of the stress response for a block of the strain history.

4.2 Simulation of Stress-Strain Response

Simulating the stress-strain response is one method to determine mean stress levels of a strain history. Martin [4] developed an analytical technique based on a combination of springs and sliders. Wetzel [5] contributed an "availability matrix" concept to this model to describe the hysteresis and cyclic memory effects most metals exhibit. The availability matrix is employed in Wetzel's model to determine what portion of the cyclic stress-strain curve is available for deformation. A detailed discussion and example of this method is given in Ref. 16.

The availability matrix concept requires the cyclic stress-strain curve be divided into a series of straight line segments. For the following analysis, the availability matrix concept is incorporated into the event identification procedure. Fifty segments are used to describe the cyclic stress-strain curve (Eq. 1).

4.3 Event Identification

Estimating the service fatigue life of a component subjected to a variable amplitude loading requires some type of algorithm to reduce the strain history into a series of constant amplitude events. Constant amplitude strain-life fatigue data can then be employed to estimate damage for the events identified. Several algorithms are available [8], including peak counting, level crossing, range counting, and rainflow counting.

In the rainflow counting procedure, the stress-strain response is analyzed to identify events that form closed hysteresis loops (Fig. 11). A strain range and mean stress level may be associated with each closed hysteresis loop. Rainflow counting has been shown to provide superior results in comparison to other cycle counting methods for a 4340 steel [17]. A simple algorithm to perform this analysis has been developed by Downing [18].

Mean stresses may be established in conjunction with the rainflow counting algorithm by associating a stress value with each strain point. When a strain event is identified, the corresponding mean stress level for that event is computed. This is illustrated in Fig. 11 where, for example, points D-E-D form a closed hysteresis loop and have stress levels shown on the stress-time diagram. The mean stress level is computed by averaging the stress level at points D and E respectively. As seen in Fig. 11, the mean stress level for event D-E-D is slightly tensile. Events F-G-F and B-C-B (Fig. 11) have the same strain range but show compressive and tensile mean stresses respectively.

4.4 Damage Analysis

Strain range, mean stress, and number of occurrences determined from rainflow counting are incorporated into a damage analysis to estimate the service fatigue life of the component. A damage parameter which assigns damage to an individual event and a damage summation technique are required to estimate service fatigue life.

Strain-life data are employed to determine the damage for each event identified by rainflow counting. The strain life equation is as follows:

$$\frac{\Delta\varepsilon}{2} = \frac{\Delta\varepsilon_e}{2} + \frac{\Delta\varepsilon_p}{2} = \frac{\sigma_f'}{E}(2N_f)^b + \varepsilon_f'(2N_f)^c \qquad (2)$$

For the case involving mean stresses, a modified version of Eq. 2 is used to determine the reversals to failure [19]:

$$\frac{\Delta\varepsilon}{2} = \frac{\Delta\varepsilon_e}{2} + \frac{\Delta\varepsilon_p}{2} = \frac{(\sigma_f'-\sigma_o)}{E}(2N_f)^b + \varepsilon_f'\left(\frac{\sigma_f'-\sigma_o}{\sigma_f'}\right)^{c/b}(2N_f)^c \qquad (3)$$

Either equation is solved iteratively to determine the reversals to failure for the given strain range. The reciprocal of this result is considered to be the damage for one occurrence of this strain level in the rainflow counted history.

Damage for each individual event is defined in a similar manner, and a method of summing the damages is required to predict service life. Several methods for summing damage are available, including Palmgren-Miner [9], Corten-Dolan [20], and other nonlinear methods [10].

For this analysis, only Miner's hypothesis will be considered. For a block of a history, Miner's hypothesis is often presented in the following form:

$$D_B = \sum_{i=1}^{k} \frac{(2N)_i}{(2N_f)_i} \tag{4}$$

The number of times that the block of history can be repeated is calculated by taking the inverse of the block damage:

$$B_f = \frac{1}{D_B} \tag{5}$$

Cycles to failure are estimated by Eq. 3 for each of three mean stress assumptions: (1) ignore mean stress effects; (2) mean stress obtained from actual tests; and (3) mean stress obtained from the predicted stress-strain response. Miner's hypothesis is then employed as the damage summation technique to compute the blocks to failure.

4.5 Local Strain Approach

The details discussed in the previous four sections are incorporated into the local strain approach. Prior to identification of events by rainflow counting, the actual block strain history that the specimen experienced are

reordered so that the absolute maximum strain level becomes the first end level. For block histories that are repeated many times before failure occurs, the absolute maximum strain excursion within the history may be used to determine the stress levels for the other strain excursions in the history. Either the monotonic or cyclic stress-strain curve may be used to determine the stress excursion for the first strain excursion. Since the histories are repeated several times, the cyclic stress-strain curve was employed to analyze the subsequent deformation. To maintain continuity, the corresponding actual stress history is also reordered to begin at the same point as the sorted strain history. This reordering does not alter the results of rainflow counting, and simplifies the algorithm required.

Damaging events for the rearranged strain history are identified by employing the rainflow counting algorithm (see section 4.3). To account for mean stresses, the rainflow counting procedure is modified to compute mean stress levels for each strain event identified. Mean stresses are determined for each event by two methods: (1) correlating a stress level to each strain level using the actual sorted stress history for the specimen; and (2) incorporating the availability method for simulation of the stress response. Equation 1 is used within the context of the availability method to model the cyclic stress-strain response of the material. Stable half-life stress-strain properties are employed in Eq. 1. Cyclic hardening, softening, or relaxation phenomena are not accounted for. The actual stress-strain response taken at various blocks of a test are used to evaluate the sensitivity of the local strain approach to this assumption.

Damage for each event identified is taken to be the reciprocal of the fatigue life for that event (Eq. 4). The zero mean stress (ZMS) fatigue life

estimates are computed, ignoring mean stress effects, from the strain life relation (Eq. 2). Incorporation of mean stresses into the analysis is accomplished by employing the modified strain life equation (Eq. 3). Damage calculated from the strain history with the actual stress response is denoted as the actual mean stress (AMS) life prediction. The strain history with the simulated stress response is analyzed, resulting in the predicted mean stress (PMS) life prediction. Regardless of the mean stress assumption, total damage for a block of the history is determined using Miner's hypothesis (Eq. 4). Predicted blocks to failure are calculated using Eq. 5.

5. SERVICE HISTORY SIMULATIONS

5.1 Test Program

Smooth specimens were subjected to the variable amplitude strain histories depicted in Figs. 3, 4 and 5. The history regeneration was accomplished by employing a microprocessor system with the histories stored in an EPROM (Eraseable Programmable Read Only Memory) which controlled an analog MTS servo-hydraulic test system. A DEC 11/34 minicomputer and an MTS 433 processor interface were used to acquire the stress-strain history which the specimen experienced. Data analysis was performed on an IBM-PC.

Preliminary evaluation of service histories indicated that a scale factor would be required to reduce test time. Scale factors of three and four times the original strain history were implemented. It is important to note that for histories A and C, only the service portion of the history was amplified (i.e., the offset strains were not amplified). Amplification of the offset strain would have resulted in their dominating the damage calculations. "Actual" stress-strain response for scale factors of one and two were obtained as follows: (1) tests were conducted at that level for approximately twenty blocks; (2) stress-strain data were collected; and (3) the specimen was tested to failure at an increased scale factor. Fatigue damage due to the loading at lower scale factors was considered insignificant in comparison to subsequent loading. By Miner's hypothesis [9], it was found that less than 2% of the damage is attributable to the lower scale blocks.

5.2 Results and Discussion

Rainflow counted strain histograms for each history at a scale factor of one are shown in Figs. 12, 13 and 14. Diagrams for every scale factor could

be provided; in fact, they differ only by a linear increment, and the same information may be extracted from the graphs mentioned above. Mean stress level changes, however, will not be proportional if plastic deformation occurred.

At a scale factor of one, the largest strain range for the three histories occurred in history A and was about 1400 microstrain. History A consists of a larger number of 300- to 900-microstrain range events in comparison to histories B and C. If large strain excursions dominate the damage, then history A would be expected to have the shortest service fatigue life.

The rainflow program combined with the availability matrix method was employed to predict mean stresses for the given strain history. A comparison of the actual and predicted mean stresses for the three histories (Figs. 15, 16 and 17), at a scale factor of one, illustrates that, while the predicted behaviors exhibit the same characteristics as the actual mean stresses, they are offset. The scale factor of one displays the most severe mean stress offset. Mean stress offset is reduced at higher scale factors due to the large amount of plasticity induced by scale amplification. The stress-strain simulation technique employed consistently provided mean stresses that resulted in non-conservative life estimates in comparison to those obtained from the measured levels. This effect is most pronounced in history A.

Actual mean stress levels for history A are seen to be in the 15- to 25-ksi range, and 5- to 15-ksi range for the predicted response. The 1000-microstrain offset introduced tensile mean stress levels for this history. If the offset strains induced this error in mean stress levels, then one would expect history B, which has no offset strains, to display similar actual and

predicted stress response. The mean stress prediction for history B (Fig. 16) does not support this speculation. This indicates that the method for simulating the stress response is not extremely accurate. The mean stress offset is not as apparent at higher scale factors, indicating that inaccuracies of the stress-strain modeling or experimental procedure caused the aforementioned discrepancy.

A comparison of the analytical and experimental results for the service fatigue life predictions for the component are given in Tables 5, 6 and 7. The results are for every specimen and each scale factor employed for history A, B and C respectively. Tables 8 and 9 present the results from a limited analysis of histories A and C without the offset strains. These will be referred to as history AX and CX respectively. As previously noted, no tests to failure were performed for scale factors of one and two due to time constraints.

Service life predictions employing the actual mean stress behavior were not significantly different from those obtained by ignoring mean stresses for scale factors of three and four. This is illustrated in Figs. 18, 19, 20 and 21 for histories A, B, C, and AX respectively. These figures also indicate that all of the predictions and experimental blocks to failure were within a factor of two. Life predictions for histories A, C and AX were longer than experimental values (i.e., nonconservative). The only exception to this was history B, for which conservative results were computed. Results from history A and AX show that the offset strain for history A is not completely responsible for the nonconservative nature of the predictions. However, it is seen that ignoring the offset strain for history A increases the service life predicted by a factor of three for a scale factor of one. Since the offset

strains only affect the mean stresses, it is expected that mean stress correction concepts will require further investigation.

The differences in service life predictions became more significant at the scale factor of one where the mean stress correction has the greatest effect on the damage calculation. This can be seen graphically in Figs. 22, 23, 24 and 25 for histories A, B, C, and AX respectively. As the scale factor is decreased, the number of blocks to failure will increase. Data on these figures are normalized with respect to the zero mean stress predictions. Possible differences due to neglecting mean stresses could be as high as 80 percent at lower scale factors. This comparison assumes that the accuracy of the mean stress correction technique and Miner's damage summation method may be extrapolated to the long life region. Guesses can be made concerning which prediction would be best for long life. This involves a degree of uncertainty because no experimental data is available to substantiate the estimates. These results should only be considered "trend lines" until long life testing can be performed.

Damage histograms are shown in Figs. 26, 27 and 28 for each of the histories (A, B, and C, respectively) at a scale factor of one. Each individual damage level is normalized to its percentage of the total amount of damage calculated by Miner's hypothesis for the respective history. These figures indicate that a majority of the damage results from only a few occurrences at the larger strain ranges. Theoretically, strain ranges below 500 microstrain could be eliminated without severely altering the service life estimate. Elimination of these excursions from the histories could be employed to investigate sequence effects. If these are not prevalent at shorter fatigue lives, perhaps this technique may be employed to shorten the

test time for long life comparisons. An indication of the effect of truncation procedures may be inferred from Socie and Artwohl [21].

6. CONCLUSIONS

The local strain approach was employed to estimate the service fatigue life for three strain histories. Mean stress corrections were incorporated into the local strain approach to obtain service fatigue life estimates ignoring mean stress, and employing predicted and experimental mean stress response of the component. Predicted service fatigue lives for the strain histories at scale factors of 3 and 4 were within a factor of two of the experimental results regardless of the mean stress correction assumption. However, there was found to be a lack of agreement between the actual and predicted stress response. Analysis indicates that this lack of correlation will become more significant at lower scale factors (i.e. longer fatigue lives). Further experimental data at the lower scale factors will be required to evaluate the effect of the mean stress.

TABLE 1

ANNEALED 1015 STEEL CHEMICAL COMPOSITION

	Specification	Actual
C	0.13/0.18	0.17
Mn	0.30/0.60	0.46
P	0.04 max	0.007
S	0.05 max	0.008
Si	0.05 max	<0.001
Cr	0.10 max	0.03
Mo	0.05 max	0.01
Ni	0.10 max	0.01
Cu	0.10 max	0.01
Sn	0.03 max	<0.001

TABLE 2

MONOTONIC TENSILE TEST CONSTANTS FOR 1015 ANNEALED STEEL

Specimen No.	12	36	Average
Hardness (BHN)	127	124	126
Modulus of Elasticity, E, $\times 10^3$ (ksi)	28.9	28.0	28.5
.2% Offset Yield Strength, $\sigma_{y.2\%}$, (ksi)	40.2	36.1	38.1
Ultimate Tensile Strength, S_u (ksi)	60.1	53.6	56.8
Percent Reduction in Area, %RA	58.8	51.6	55.2
True Fracture Strength, σ_f/σ_f^* (ksi)	126/112	90.9/82.4	108
True Fracture Ductility, ε_f	.887	.725	.806
Strain Hardening Exponent, n	.223	.225	.224
Strength Coefficient, K (ksi)	109	97.5	103

σ_f^* is the true fracture strength corrected for triaxial stress due to necking as proposed by Bridgman (22).

TABLE 3

FATIGUE LIFE TEST DATA

ANNEALED 1015 STEEL ROUND SPECIMENS

Specimen No.	$\Delta\varepsilon/2$	$2N_f$	$\Delta\bar{\sigma}/2$ (ksi)	$\Delta\bar{\varepsilon}_e/2$	$\Delta\bar{\varepsilon}_p/2$
R-32	.0100	2,174	49.5	.00160	.00840
R-35	.0080	2,246	48.5	.00162	.00638
R-20	.0070	3,034	42.8	.00142	.00558
R-34	.0040	15,880	39.0	.00127	.00273
R-22	.0030	27,460	33.9	.00114	.00186
R-25	.0020	106,700	29.5	.00094	.00106
R-19	.0018	171,700	27.6	.00093	.00087
R-37	.0014	536,500	26.2	.00087	.00053
R-24	.0012	426,200	25.3	.00084	.00036
*R-10	.0010	9,109,000	24.5	.00080	.00020

*Indicates run-out.

Note: All tests are fully reversed (i.e., $R_\varepsilon = -1$) constant amplitude strain control.

TABLE 4

CYCLIC STRESS-STRAIN AND STRAIN-LIFE CONSTANTS FOR 1015 ANNEALED STEEL

	Round
Cyclic Strength Coefficient, K' (ksi)	146
Cyclic Strain Hardening Exponent, n'	.229
Fatigue Strength Coefficient, σ_f' (ki)	113
Fatigue Ductility Coefficient, ε_f'	.355
Fatigue Strength Exponent, b	-.116
Fatigue Ductility Exponent, c	-.507
Transition Fatigue Life, $2N_f$ (Reversals)	1.00×10^5

TABLE 5

SERVICE FATIGUE LIFE IN BLOCKS TO FAILURE

STRAIN HISTORY A

Scale Factor	Specimen No.	Block σ-ε Data Taken On	Zero Mean Stress	Actual Mean Stress	Predicted Mean Stress	Experimental
1	65	1	166,230	57,057	88,196	-
	67	3	206,841	64,423	106,774	-
	67	10	195,883	62,839	97,627	-
2	68	3	6,198	5,018	4,467	-
	68	7	5,695	4,964	4,224	-
3	49	1	371	370	370	378
	52	-	-	-	-	259
	67	18	566	566	472	258
	67	135	551	463	549	258
4	65	1	125	125	111	87
	47	-	-	-	-	93
	50	-	-	-	-	77
	68	4	160	160	140	111
	68	19	220	220	192	111

TABLE 6

SERVICE FATIGUE LIFE IN BLOCKS TO FAILURE

STRAIN HISTORY B

Scale Factor	Specimen No.	Block σ-ε Data Taken On	Zero Mean Stress	Actual Mean Stress	Predicted Mean Stress	Experimental
1	81	1	215,555	114,650	187,449	-
	81	3	295,440	152,431	255,241	-
2	69	3	5,763	5,702	5,481	-
	69	30	4,748	4,706	4,478	-
3	80	1	927	947	922	1,700
	80	1,000	803	884	1,211	1,700
	53	-	-	-	-	874
	40	-	-	-	-	1,047
4	81	1	326	336	385	367
	43	-	-	-	-	282
	56	-	-	-	-	391
	69	10	245	249	244	378
	69	210	254	259	252	378

TABLE 7

SERVICE FATIGUE LIFE IN BLOCKS TO FAILURE

STRAIN HISTORY C

Scale Factor	Specimen No.	Block σ-ε Data Taken On	Zero Mean Stress	Actual Mean Stress	Predicted Mean Stress	Experimental
1	79	1	322,478	445,995	376,669	-
	64	4	361,131	593,436	441,566	-
2	62	3	4,905	5,042	5,000	-
3	62	2	670	683	674	584
	71	2	831	861	830	454
4	79	1	270	274	270	180
	79	28	251	254	245	180
	64	2	265	269	265	185

TABLE 8

SERVICE FATIGUE LIFE IN BLOCKS TO FAILURE

STRAIN HISTORY AX

Scale Factor	Specimen No.	Block σ-e Data Taken On	Zero Mean Stress	Actual Mean Stress	Predicted Mean Stress	Experimental
1	77	3	377,837	168,011	295,310	-
	77	104	372,673	124,773	295,241	-
2	77	10	4,807	4,612	4,209	-
3	63	4	356	383	325	245
	63	15	387	395	524	245
	51	-	-	-	-	184
4	44	-	-	-	-	135
	66	-	-	-	-	74
	77	4	129	130	120	107

TABLE 9

SERVICE FATIGUE LIFE IN BLOCKS TO FAILURE

STRAIN HISTORY CX

Scale Factor	Specimen No.	Block σ-ε Data Taken On	Zero Mean Stress	Actual Mean Stress	Predicted Mean Stress	Experimental
1	72	2	396,537	241,233	340,588	-
4	72	2	235	239	228	233

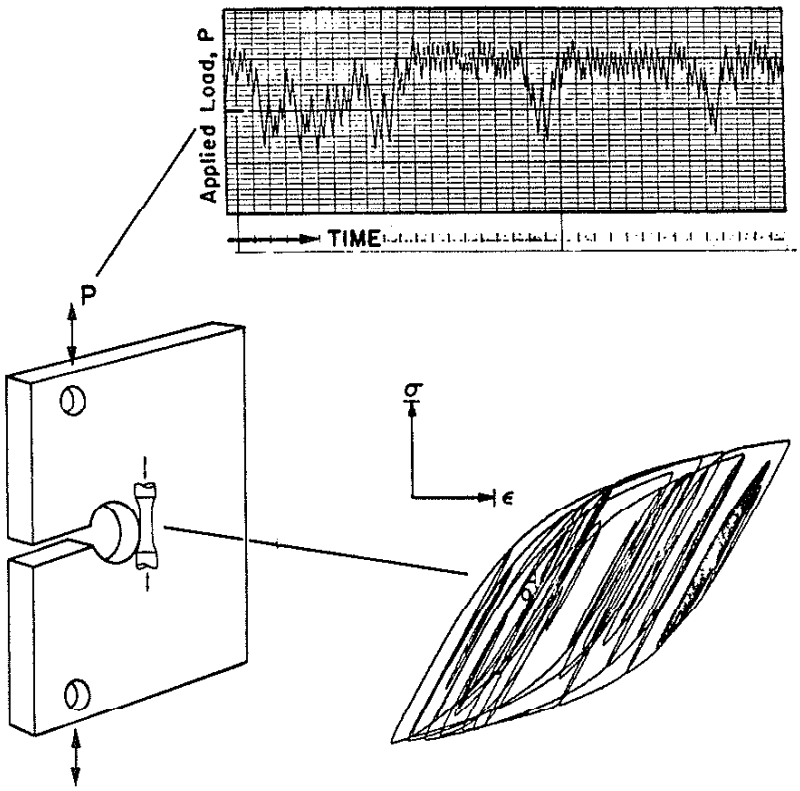

FIG. 1 LOCAL STRESS-STRAIN APPROACH TO FATIGUE ANALYSIS (REF. 2)

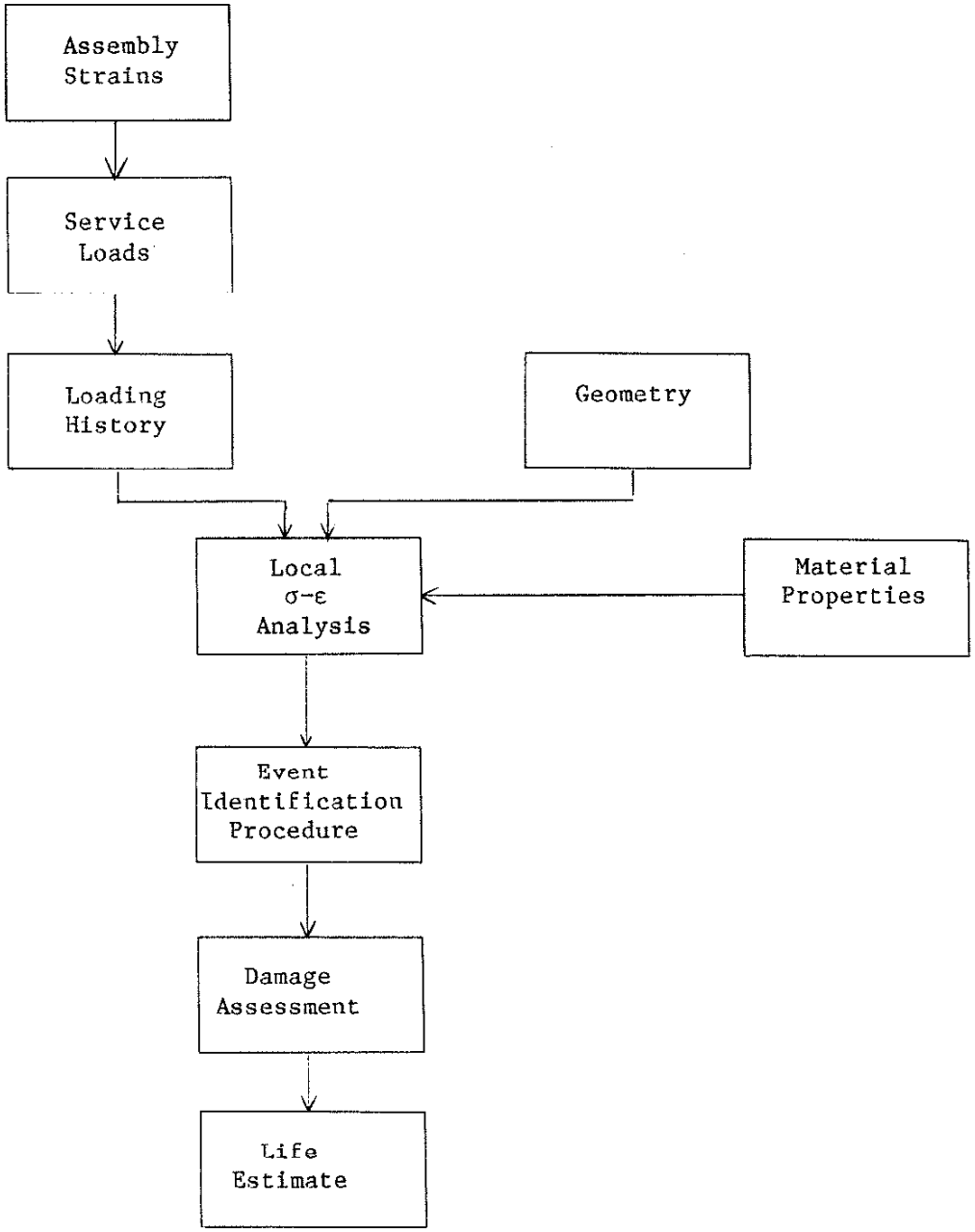

FIG. 2 FLOWCHART OF THE LOCAL STRAIN APPROACH

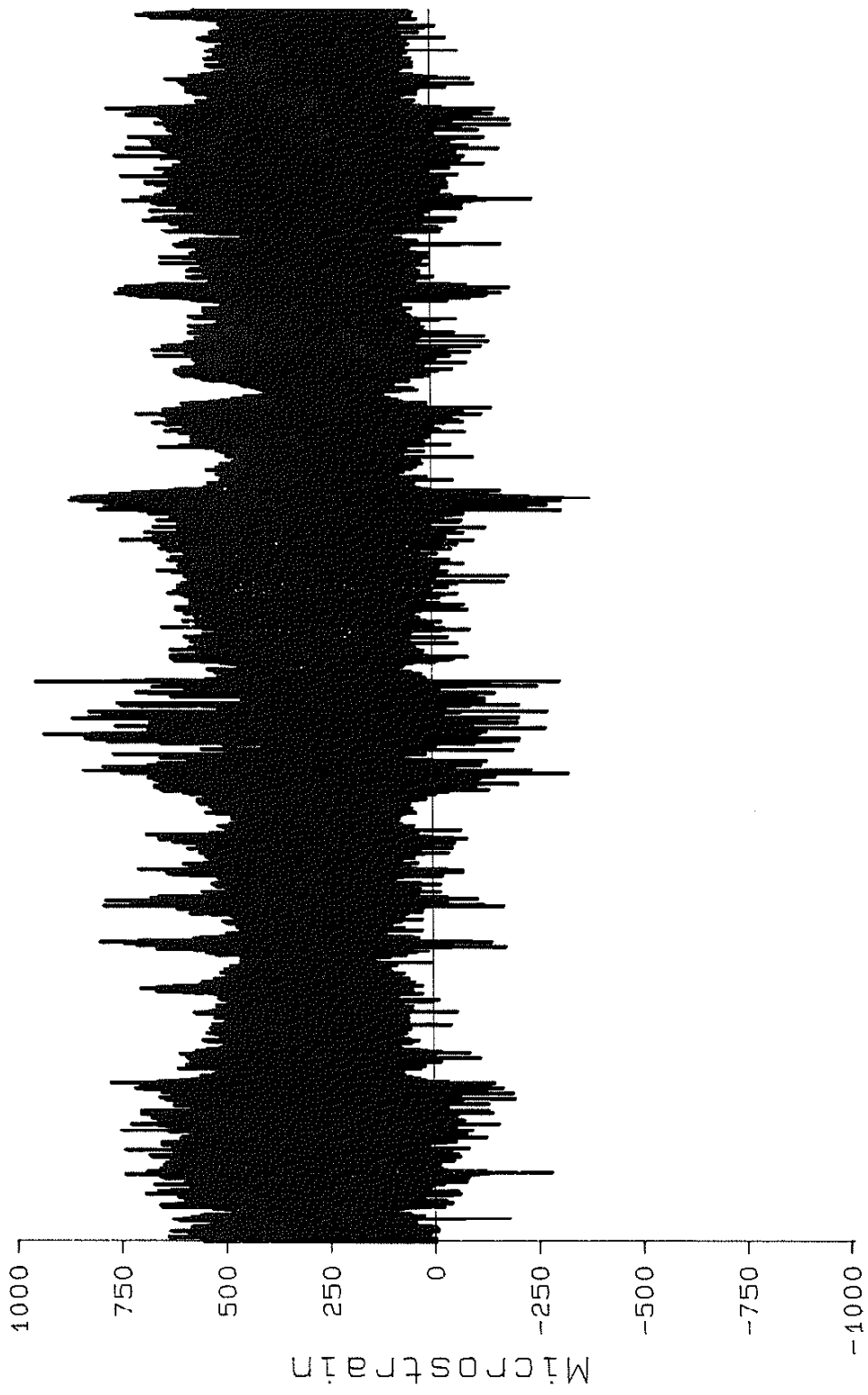

FIG. 3 HISTORY A WITHOUT 1000με OFFSET

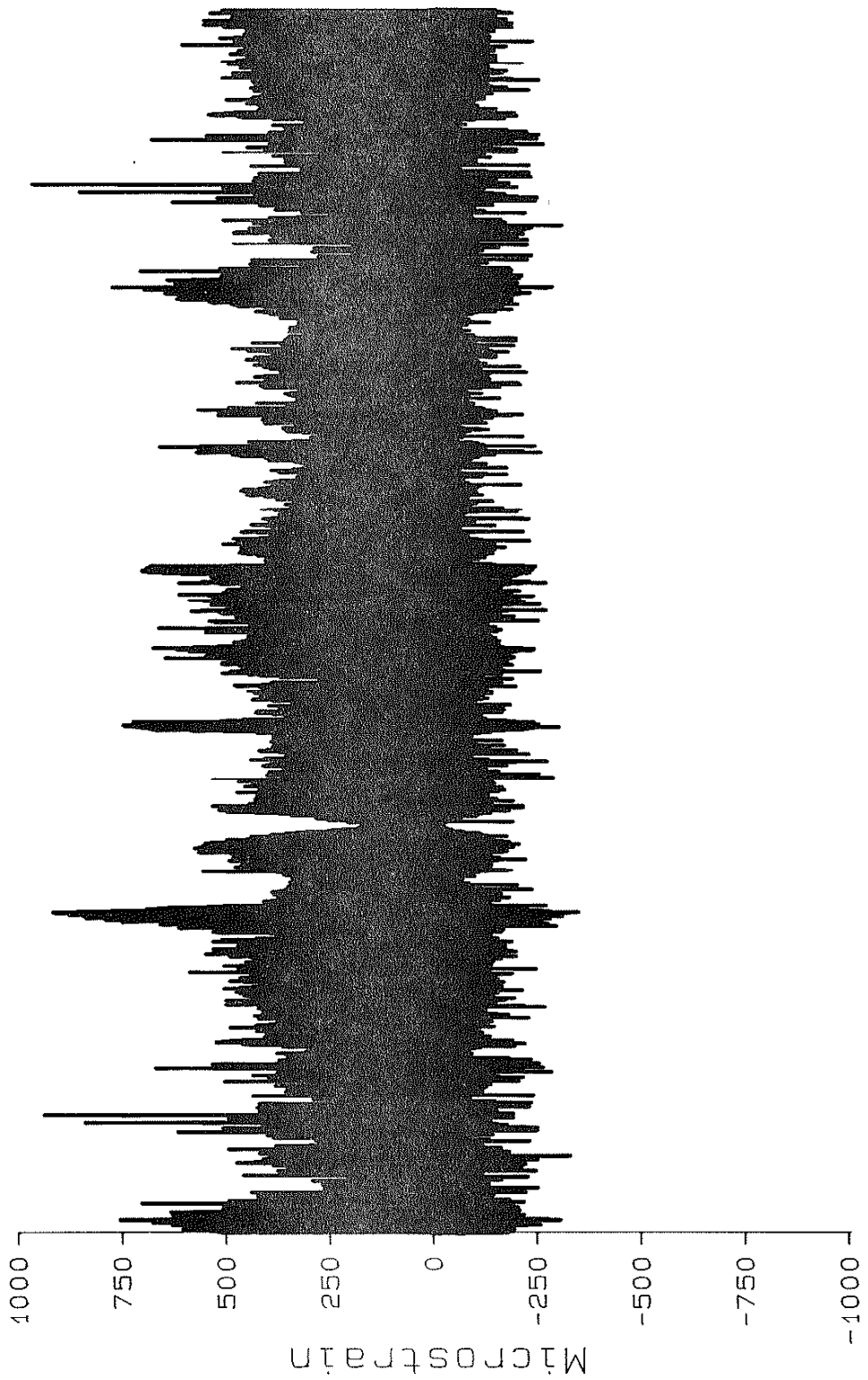

FIG. 4 HISTORY B (NO OFFSET)

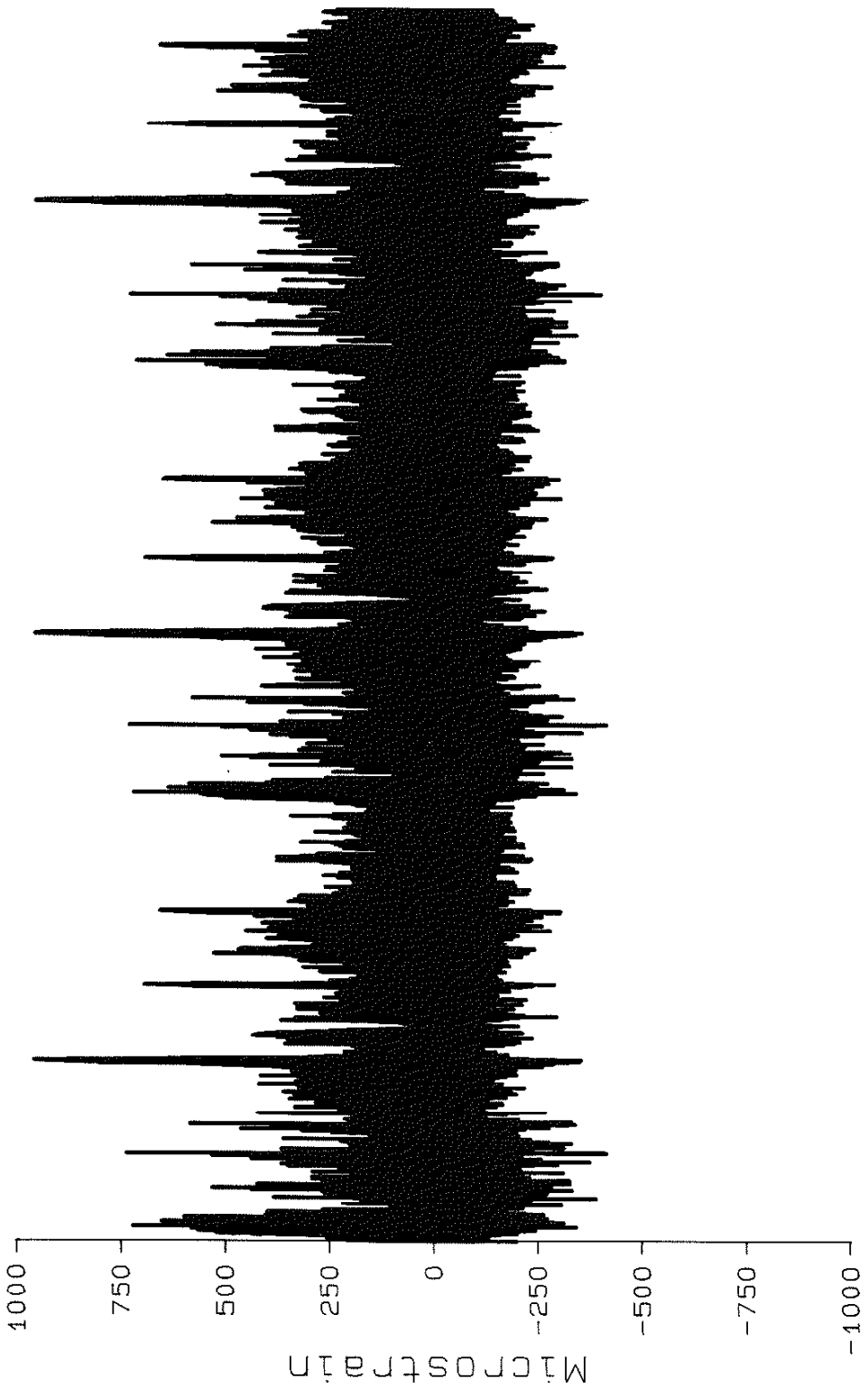

FIG. 5 HISTORY C WITHOUT -400με OFFSET

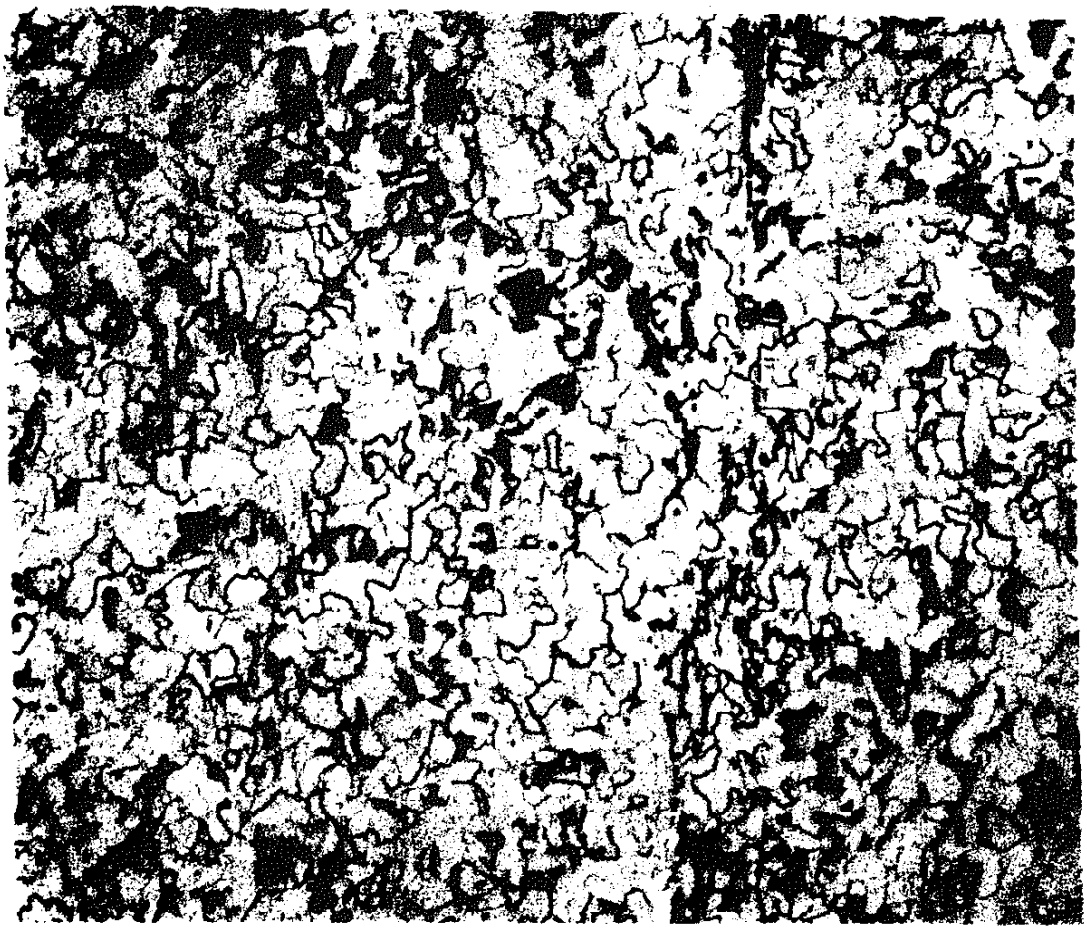

FIG. 6 MICROSTRUCTURE OF ANNEALED 1015 STEEL

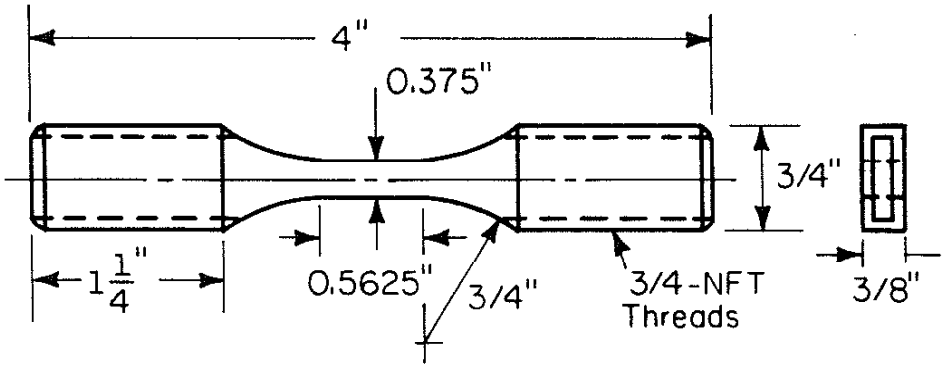

Flat Specimen

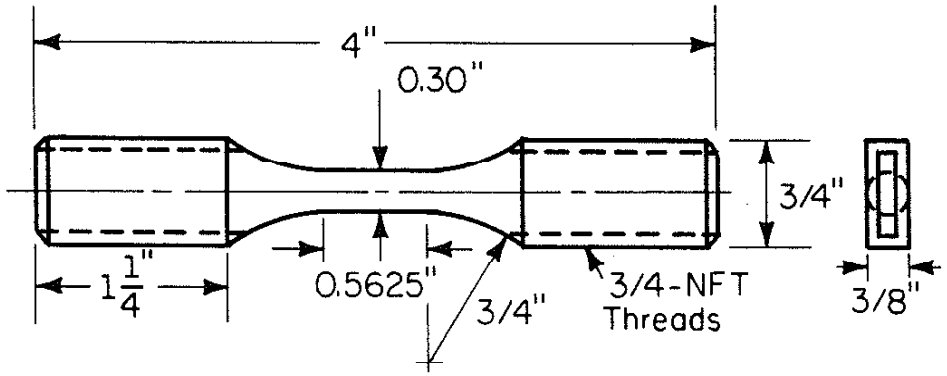

Round Specimen

600μ Finish in Gage Section

FIG. 7 SPECIMEN SPECIFICATIONS

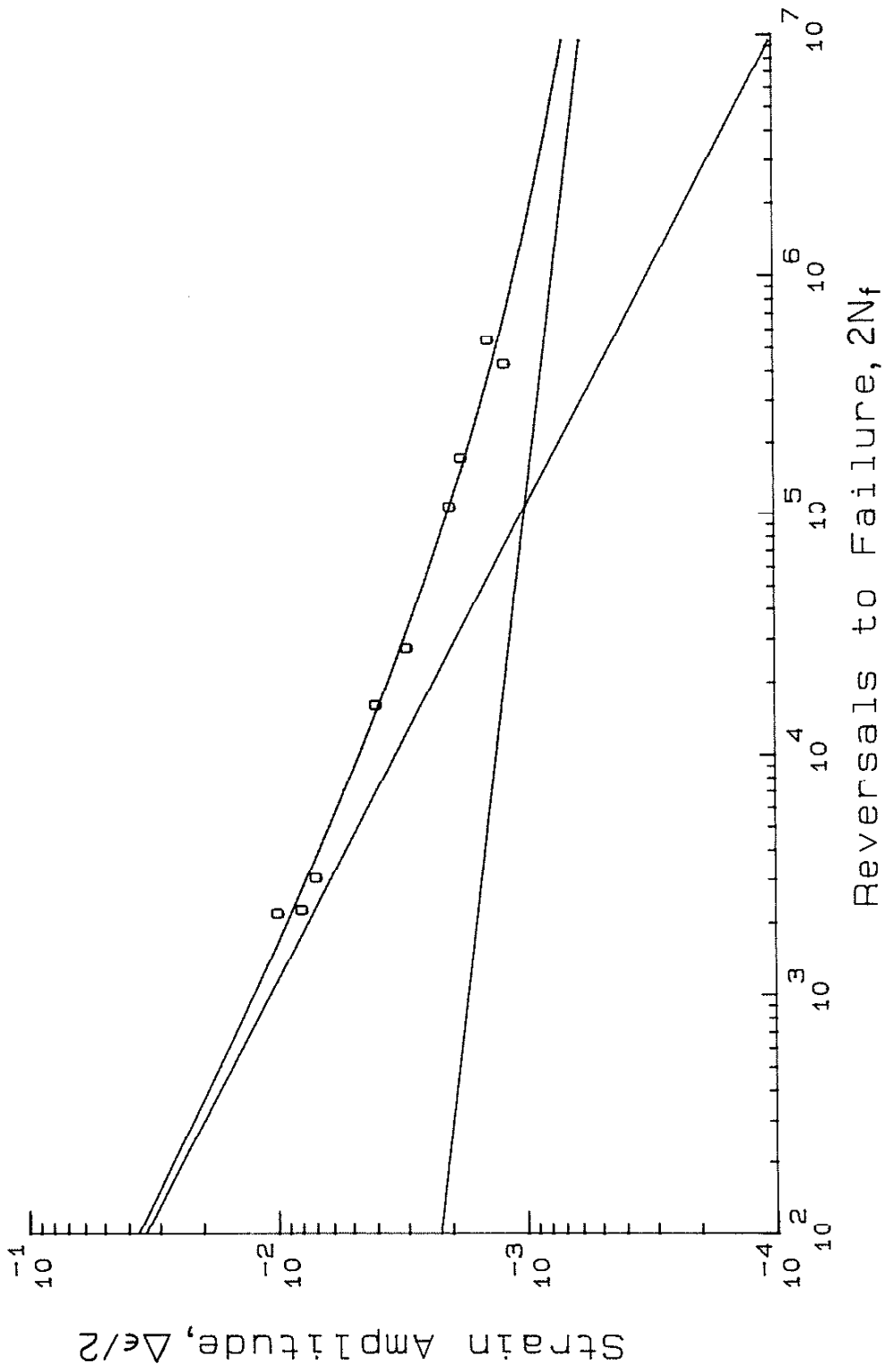

FIG. 8 STRAIN-LIFE DATA

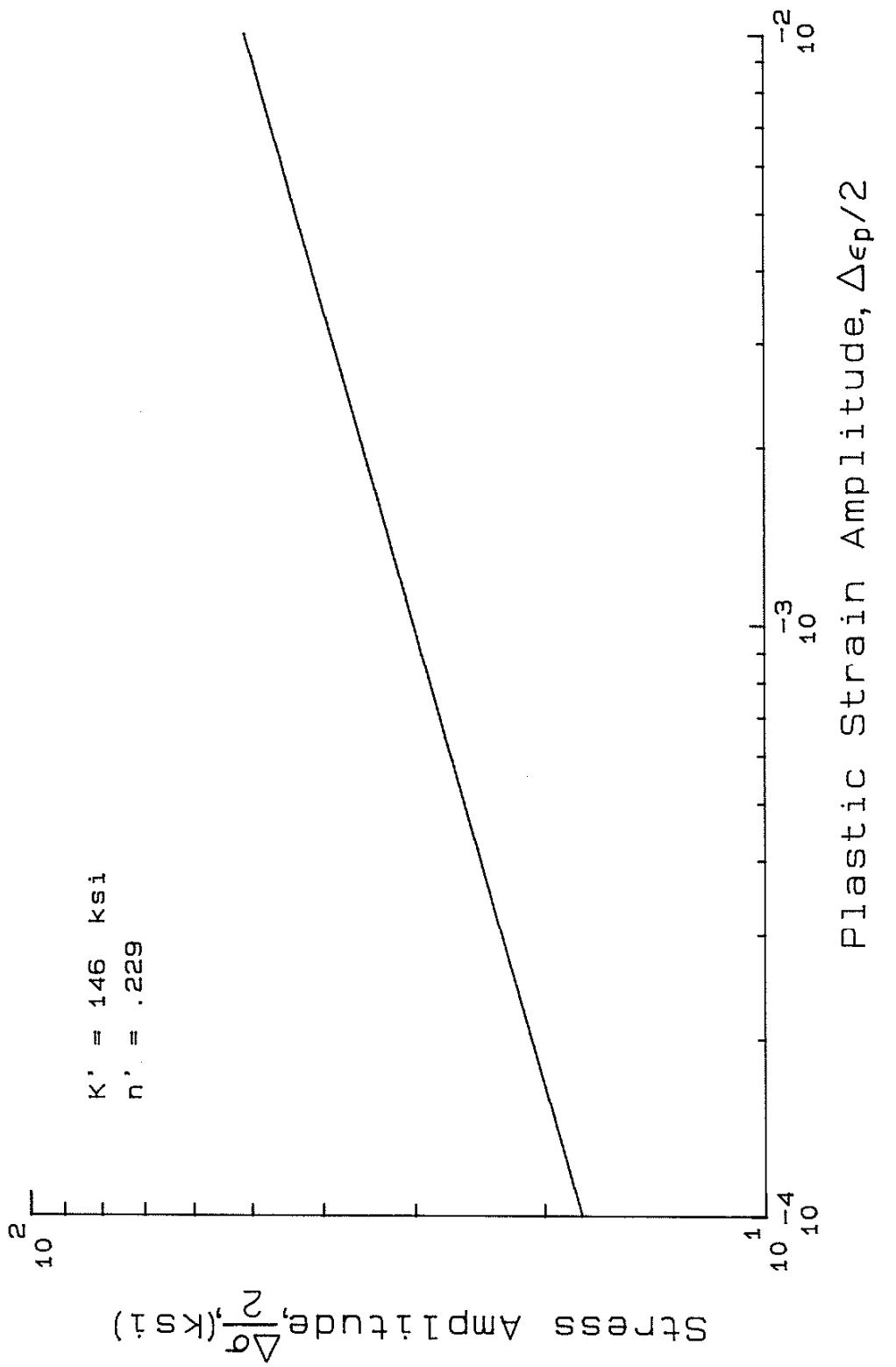

FIG. 9 CYCLIC STRAIN HARDENING COEFFICIENTS

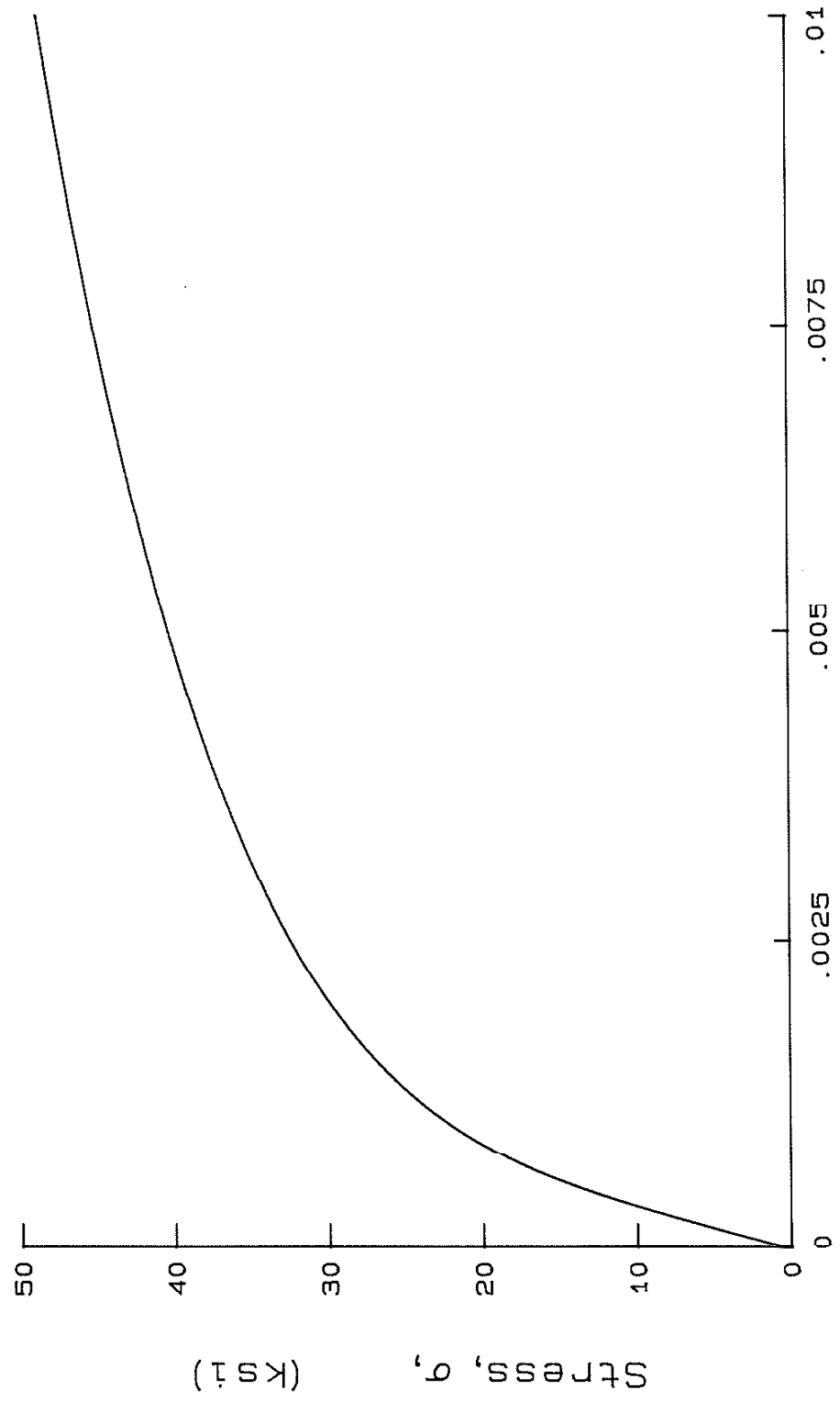

FIG. 10 CYCLIC STRESS-STRAIN CURVE

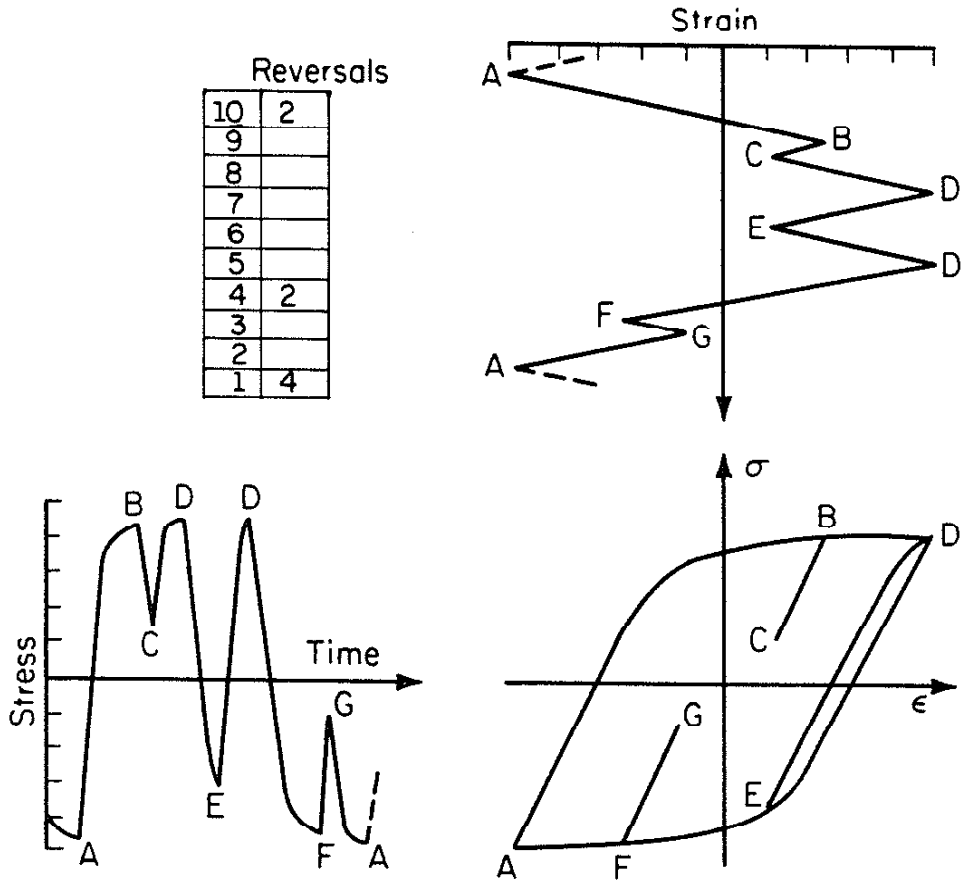

FIG. 11 RAINFLOW COUNTING ILLUSTRATION (REF. 18)

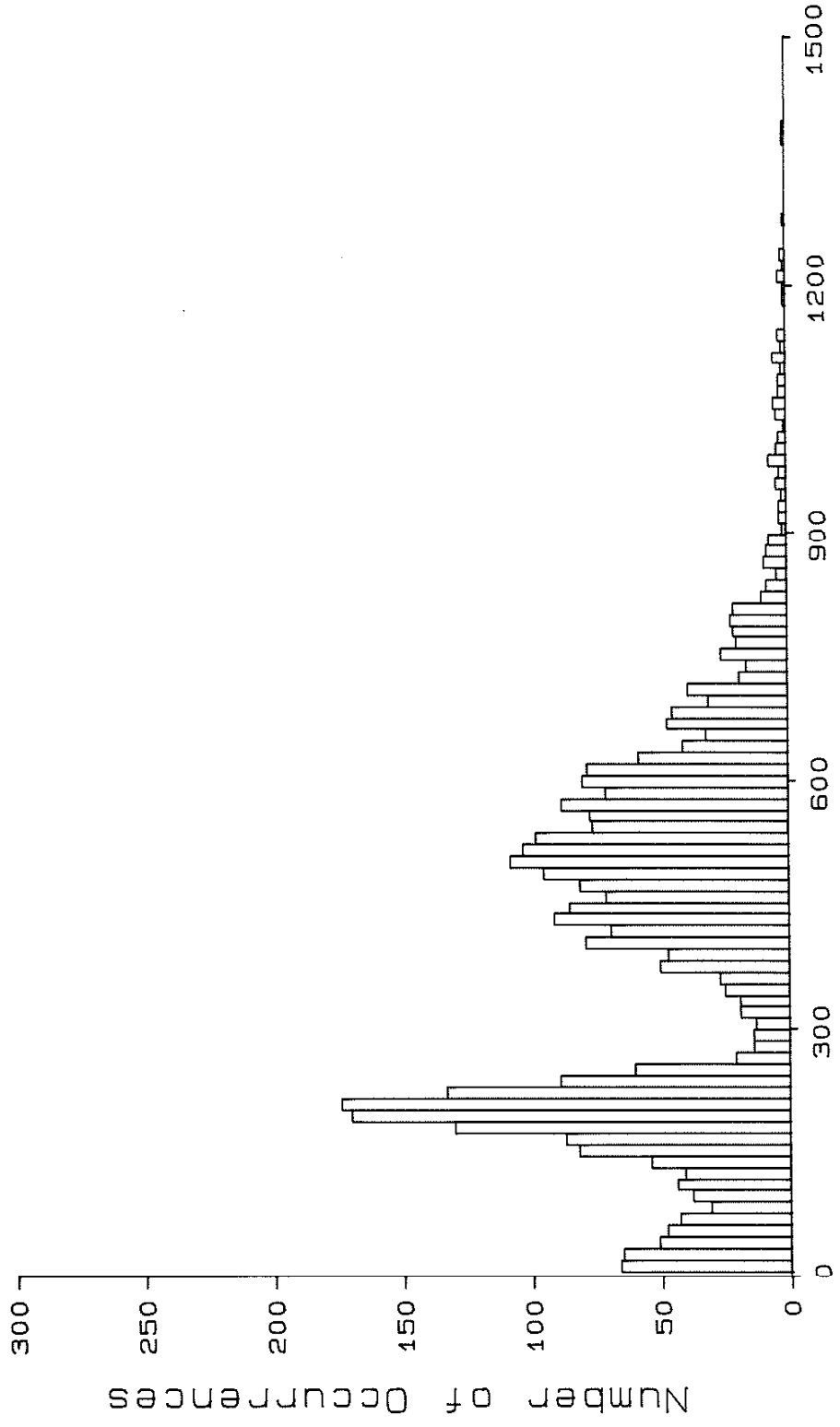

FIG. 12 HISTOGRAM FOR STRAIN HISTORY A

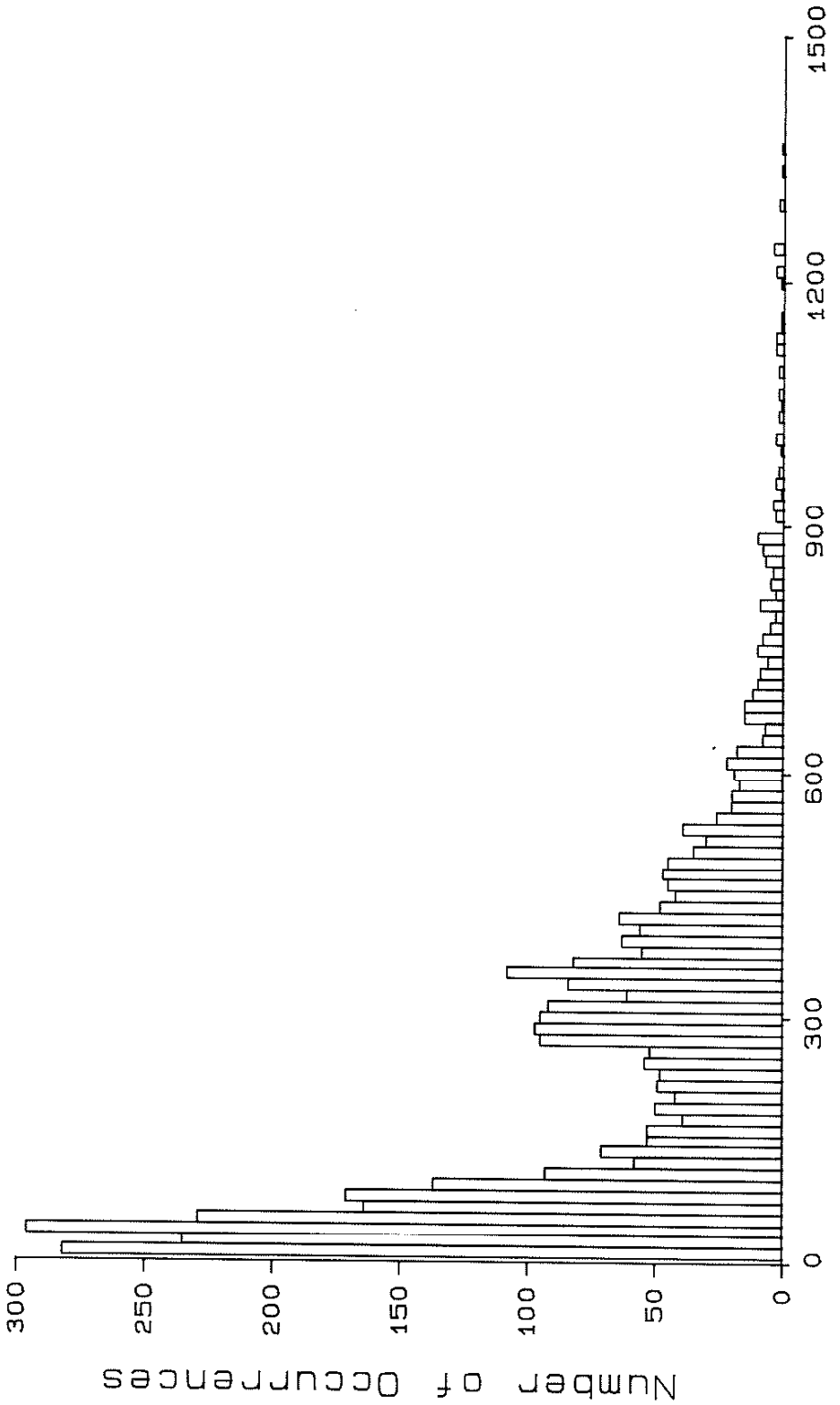

FIG. 13 HISTOGRAM FOR STRAIN HISTORY B

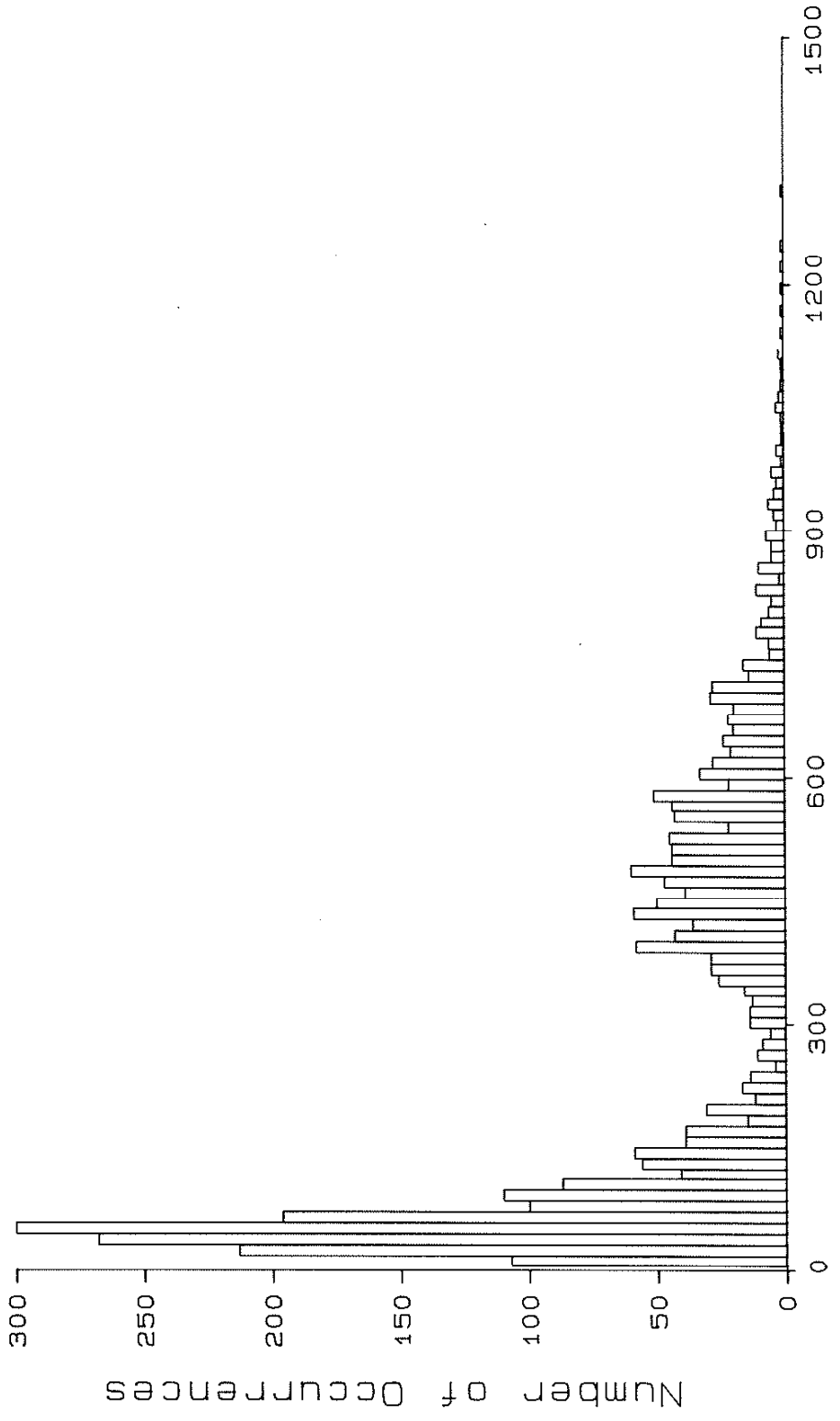

FIG. 14 HISTOGRAM FOR STRAIN HISTORY C

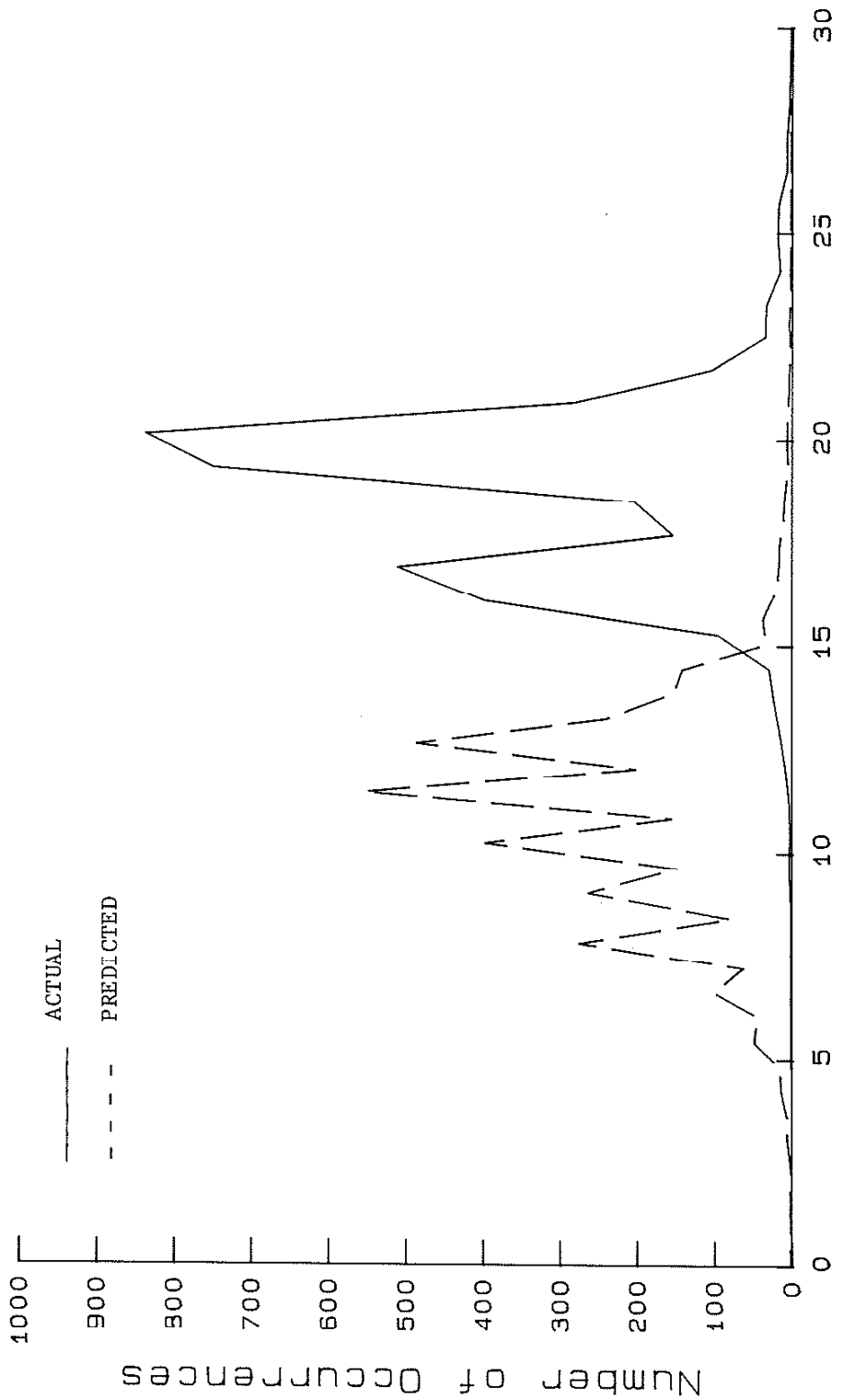

FIG. 15 COMPARISON OF CALCULATED AND MEASURED MEAN STRESS, HISTORY A

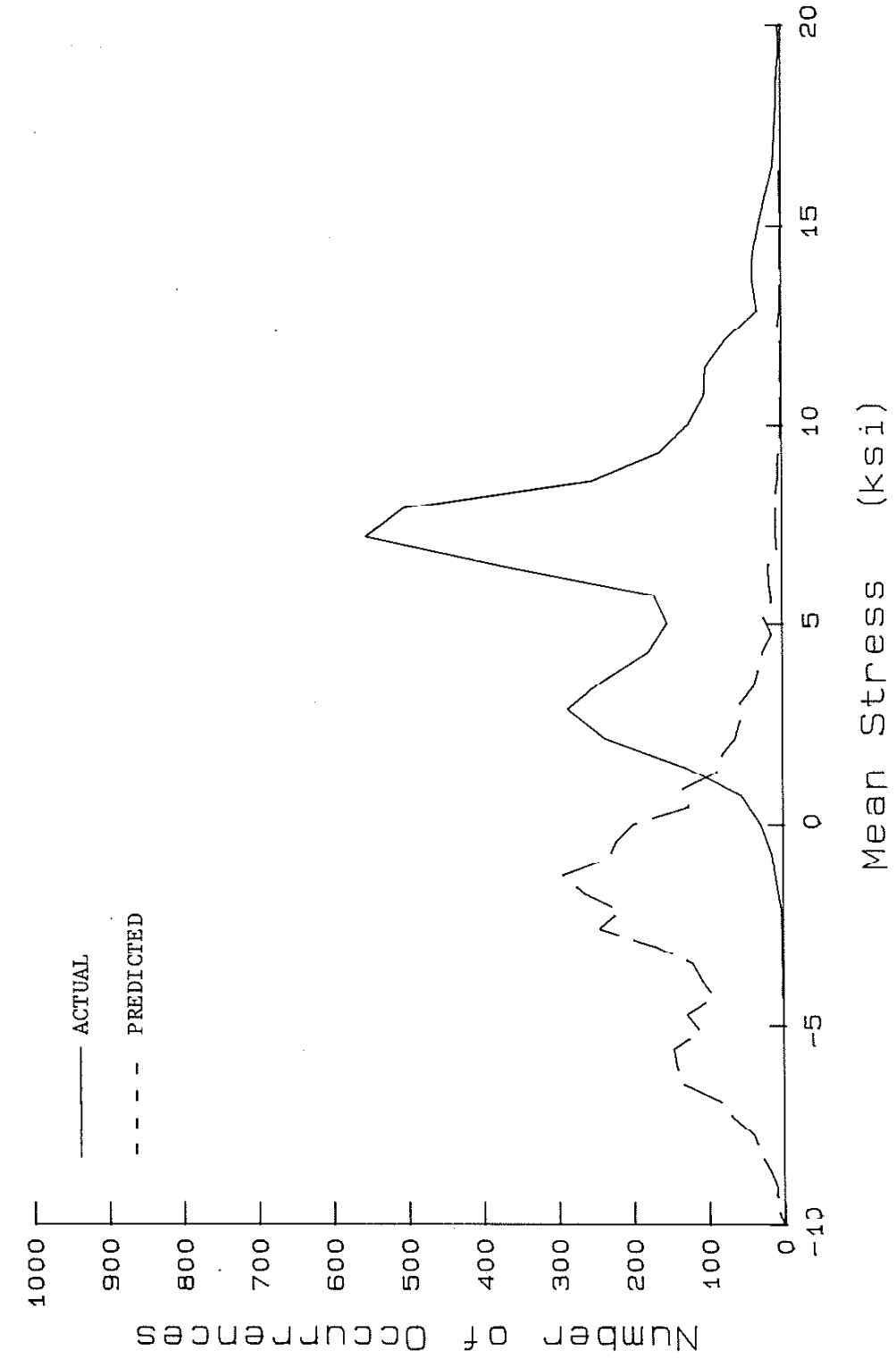

FIG. 16 COMPARISON OF CALCULATED AND MEASURED MEAN STRESS, HISTORY B

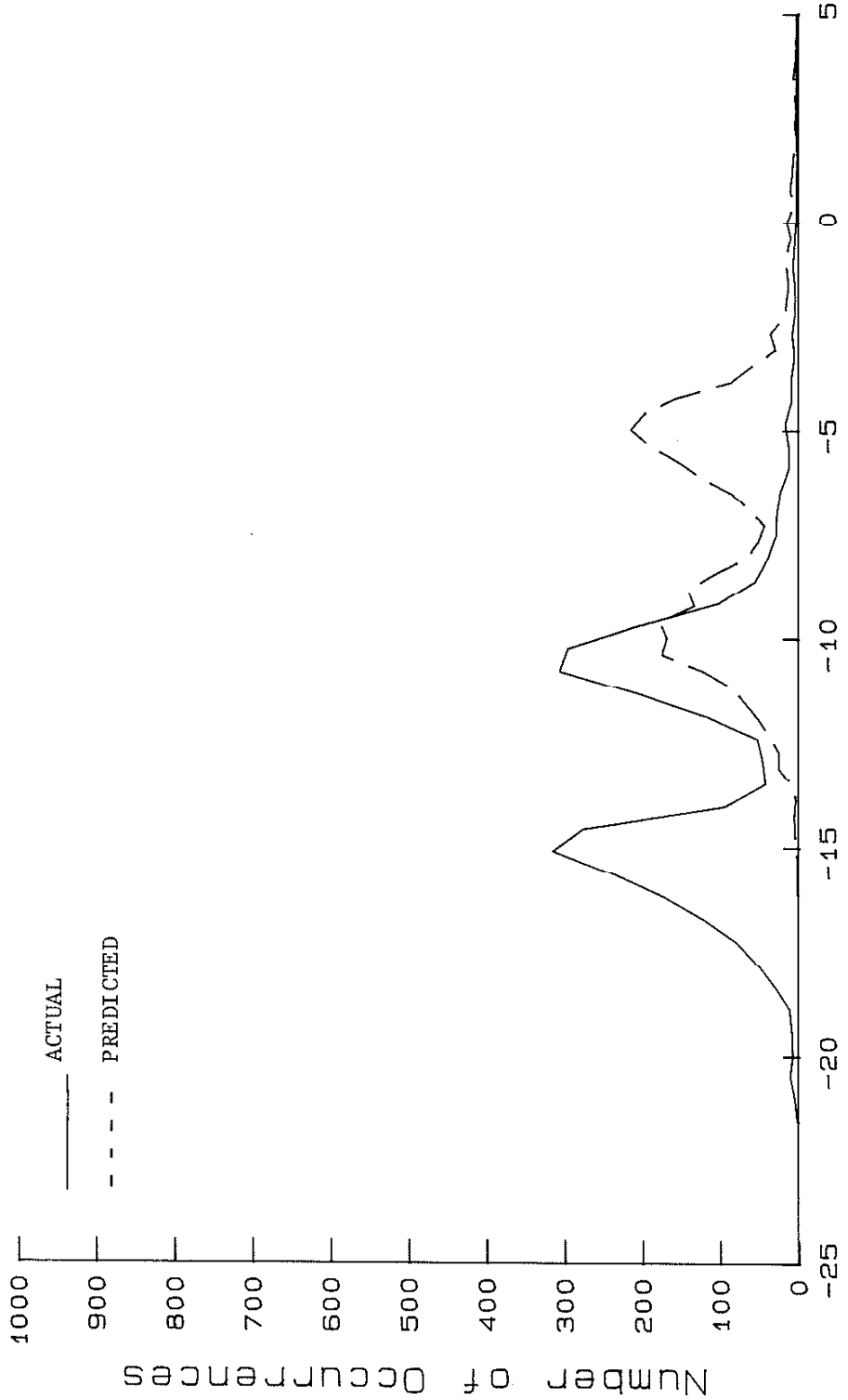

FIG. 17 COMPARISON OF CALCULATED AND MEASURED MEAN STRESS, HISTORY C

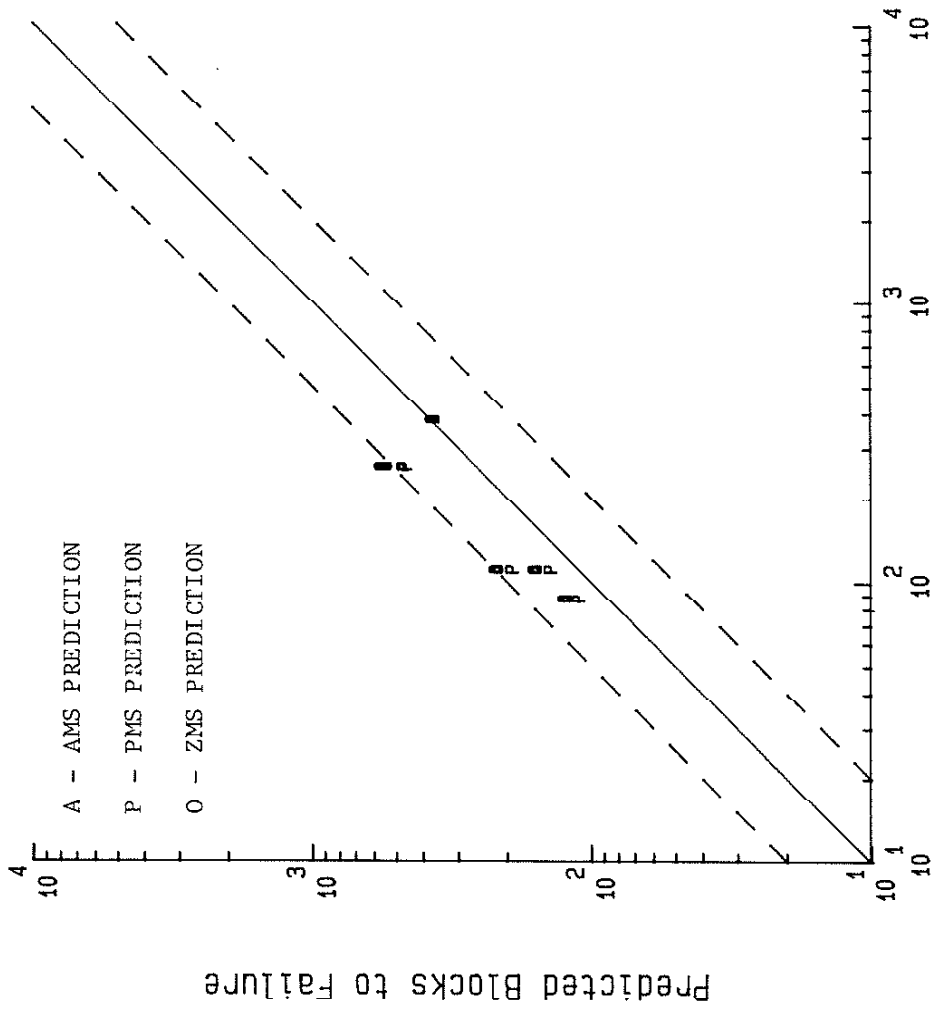

FIG. 18 PREDICTED VS. EXPERIMENTAL BLOCKS TO FAILURE, HISTORY A

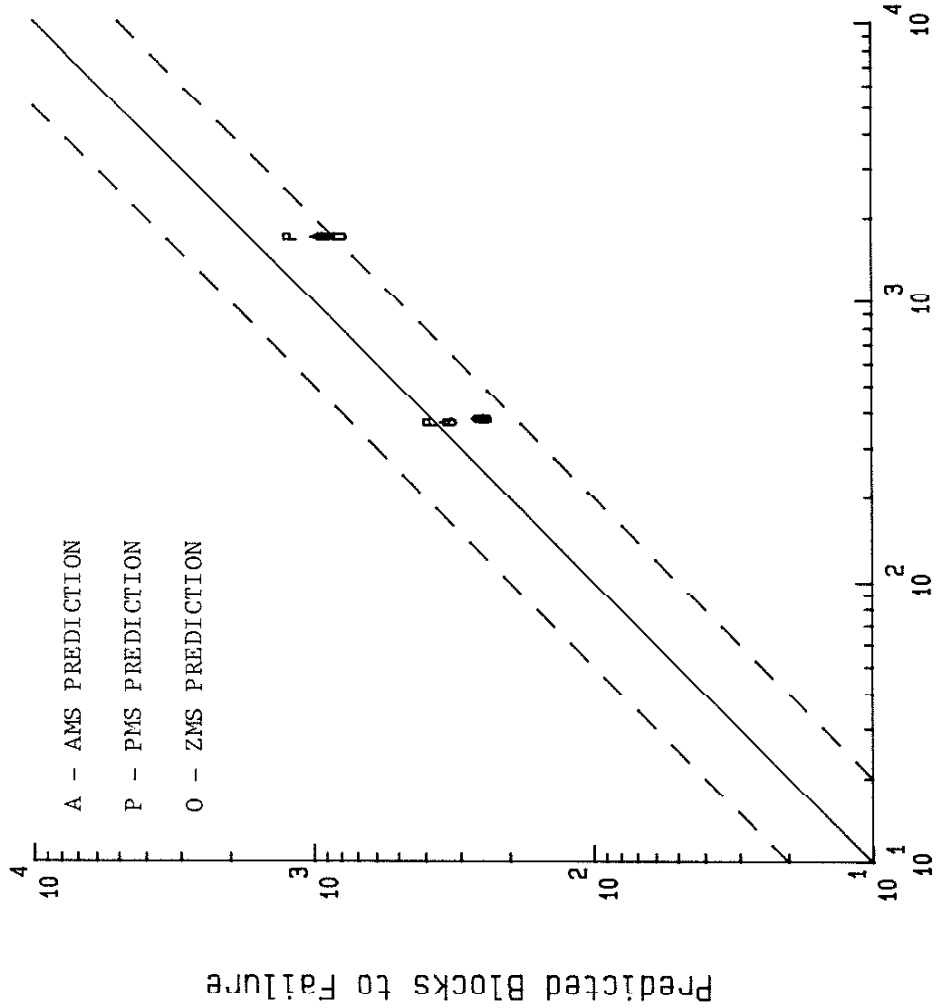

FIG. 19 PREDICTED VS. EXPERIMENTAL BLOCKS TO FAILURE, HISTORY B

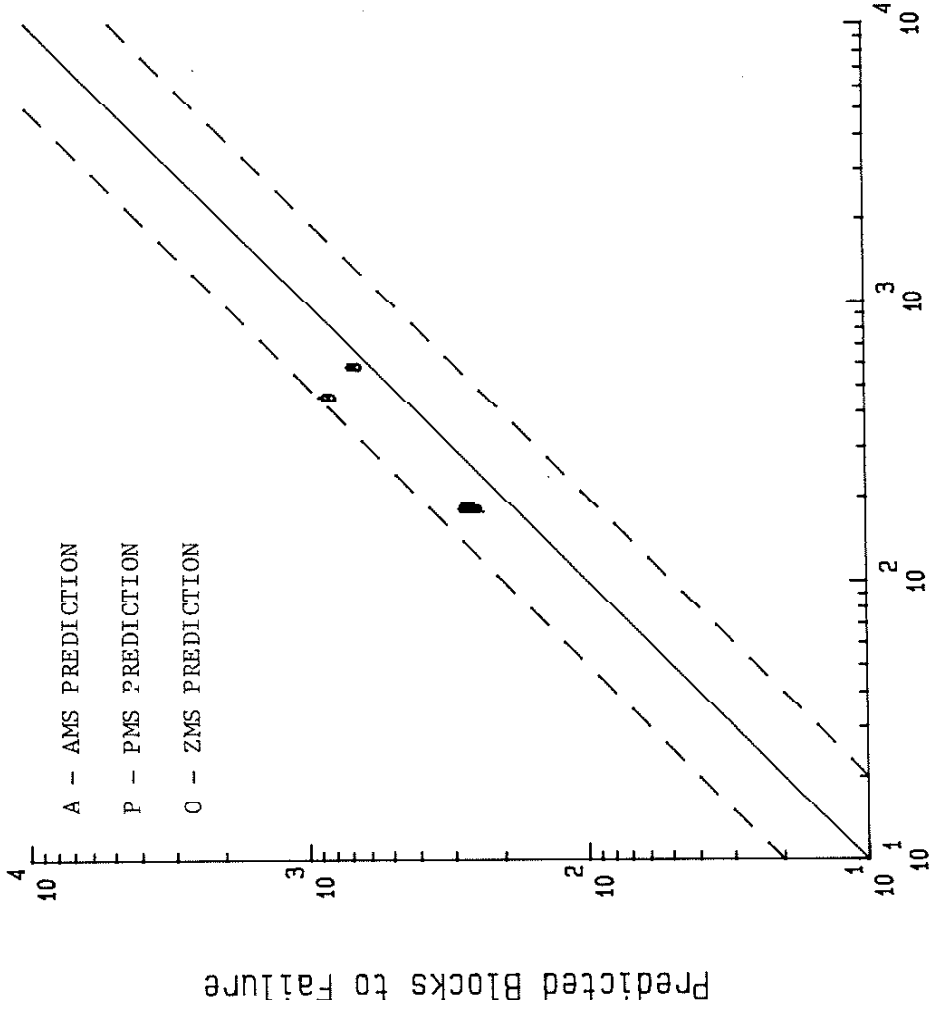

FIG. 20 PREDICTED VS. EXPERIMENTAL BLOCKS TO FAILURE, HISTORY C

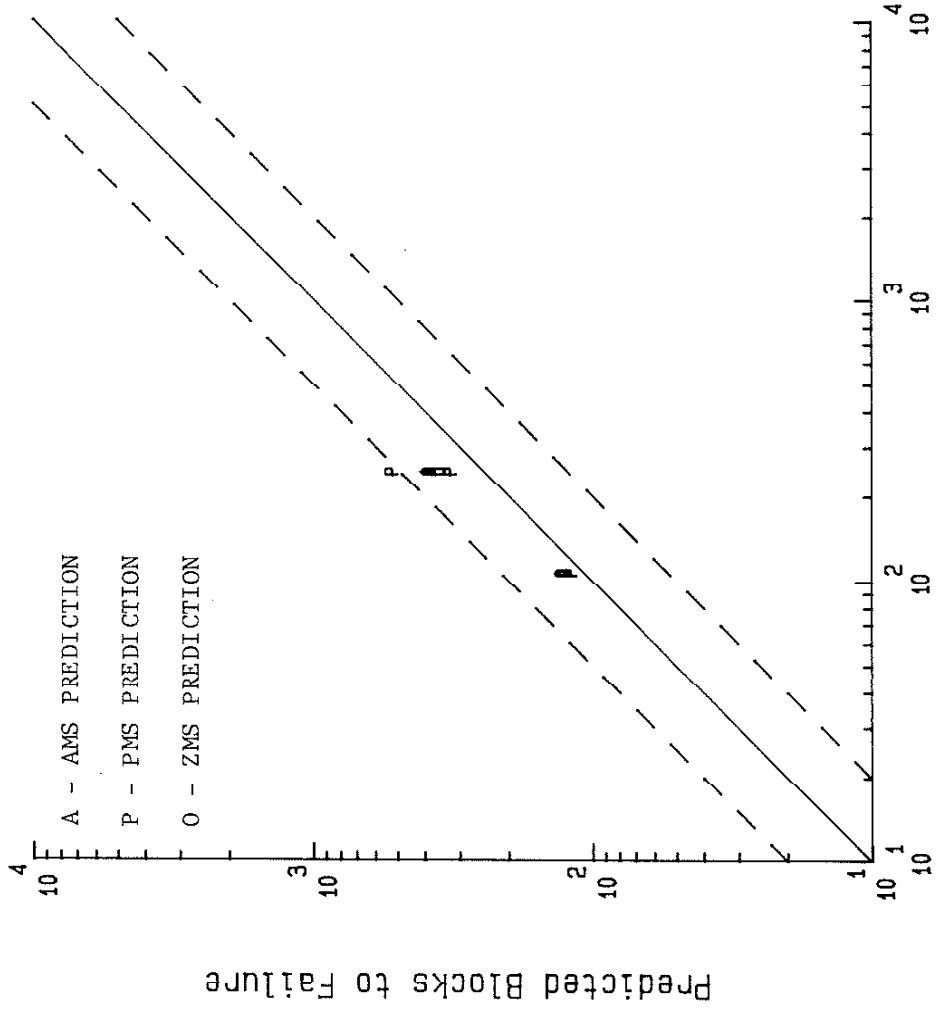

FIG. 21 PREDICTED VS. EXPERIMENTAL BLOCKS TO FAILURE, HISTORY AX

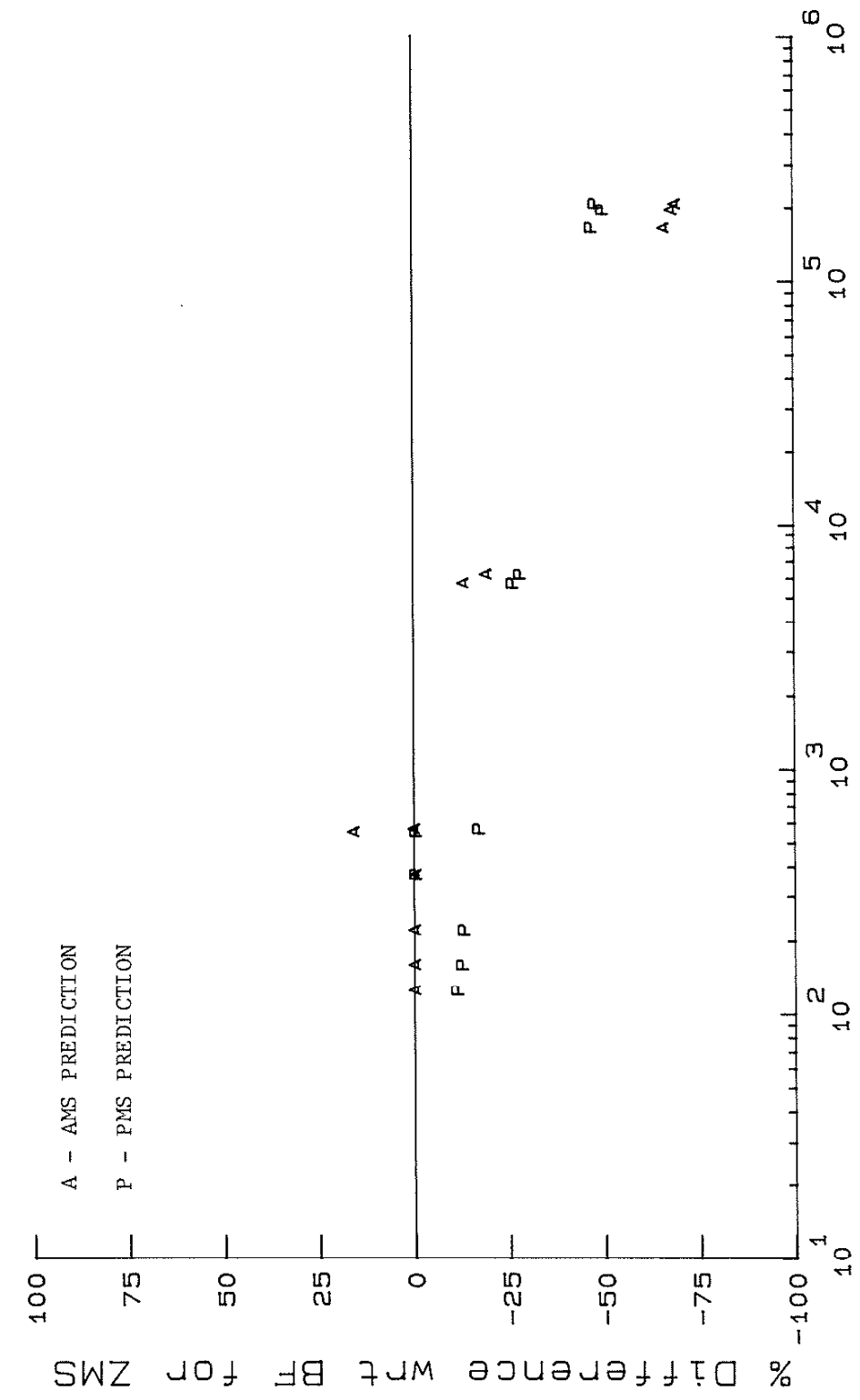

FIG. 22 COMPARISON OF MEAN STRESS PREDICTION METHODS, HISTORY A

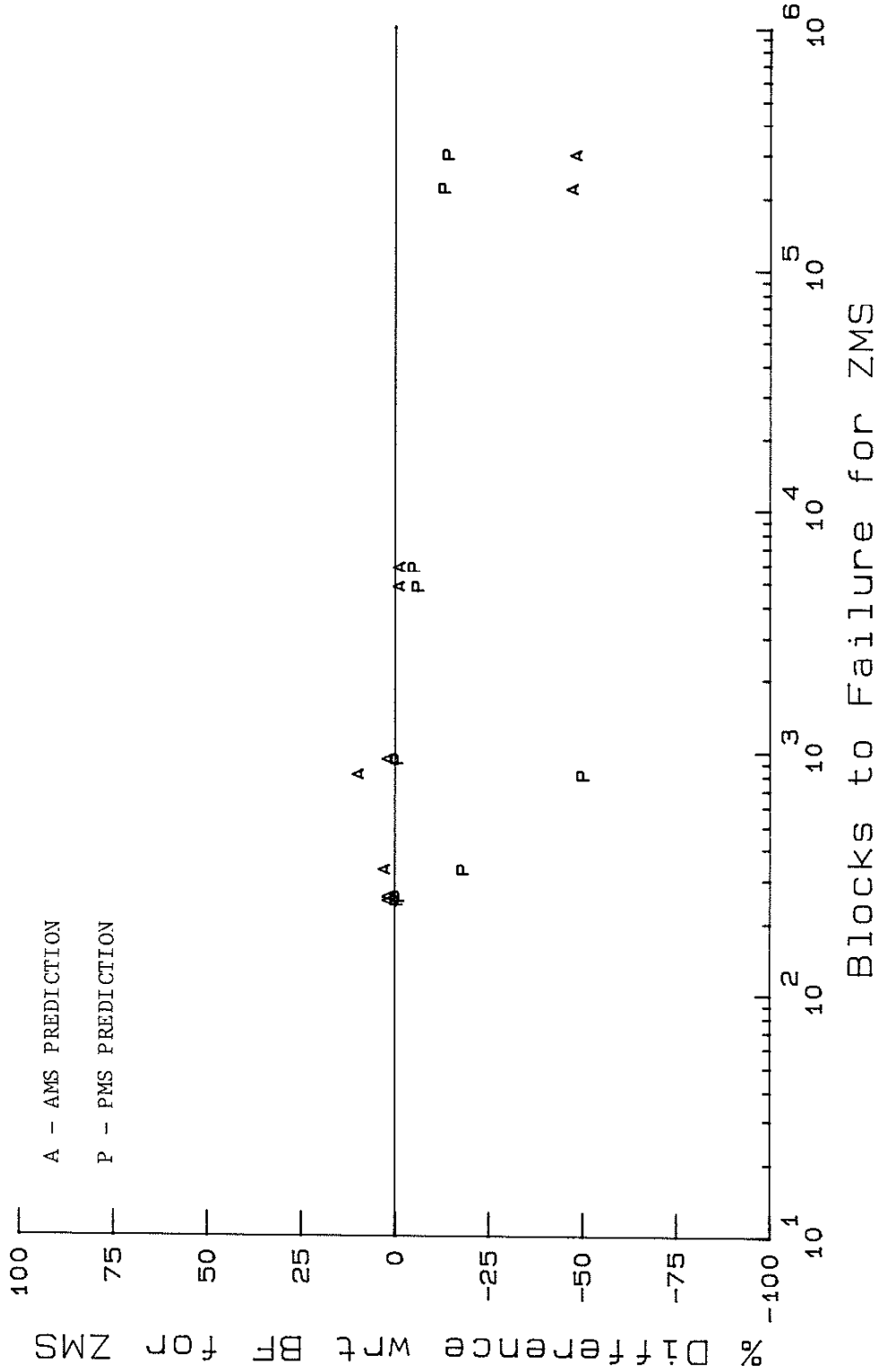

FIG. 23 COMPARISON OF MEAN STRESS PREDICTION METHODS, HISTORY B

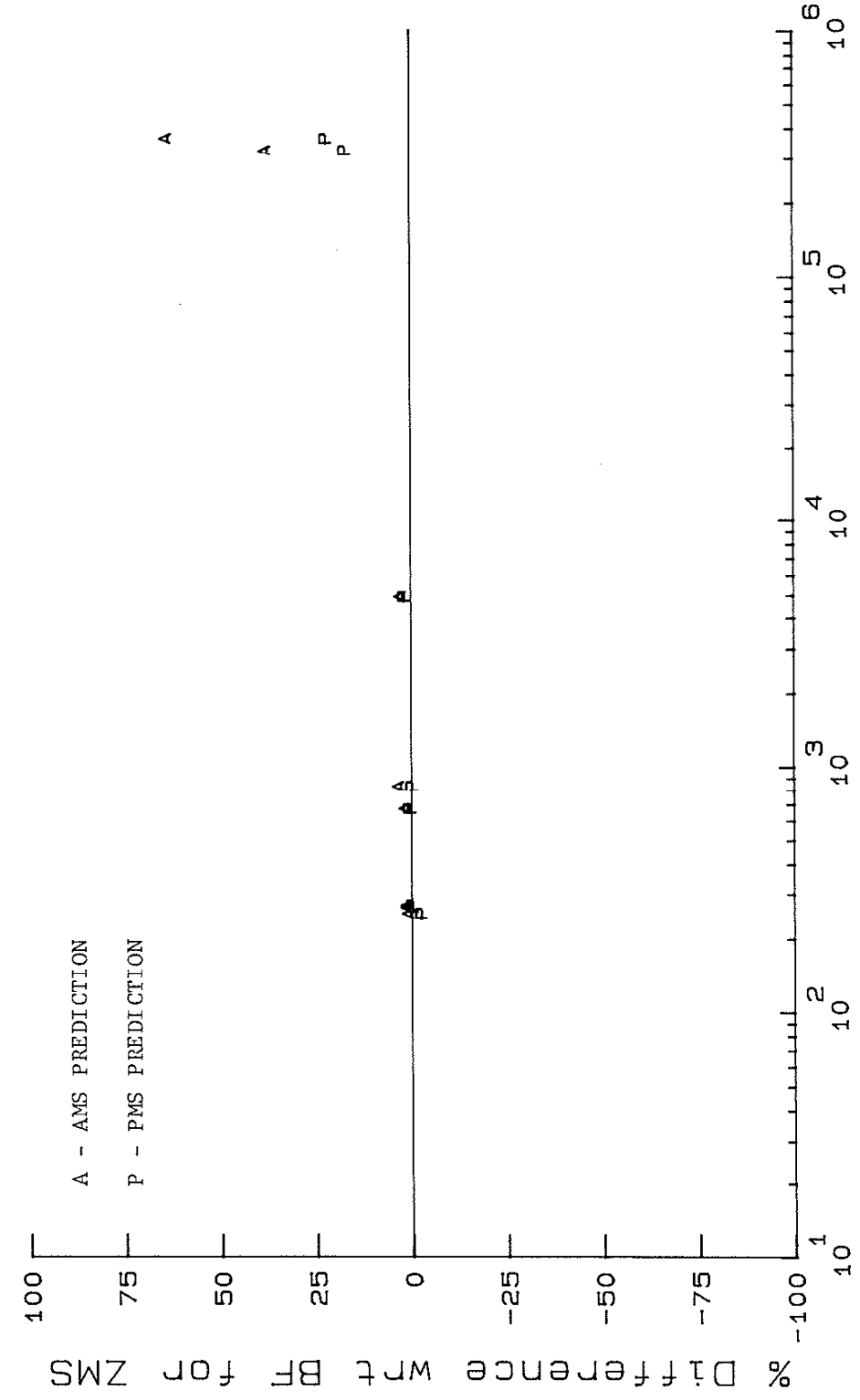

FIG. 24 COMPARISON OF MEAN STRESS PREDICTION METHODS, HISTORY C

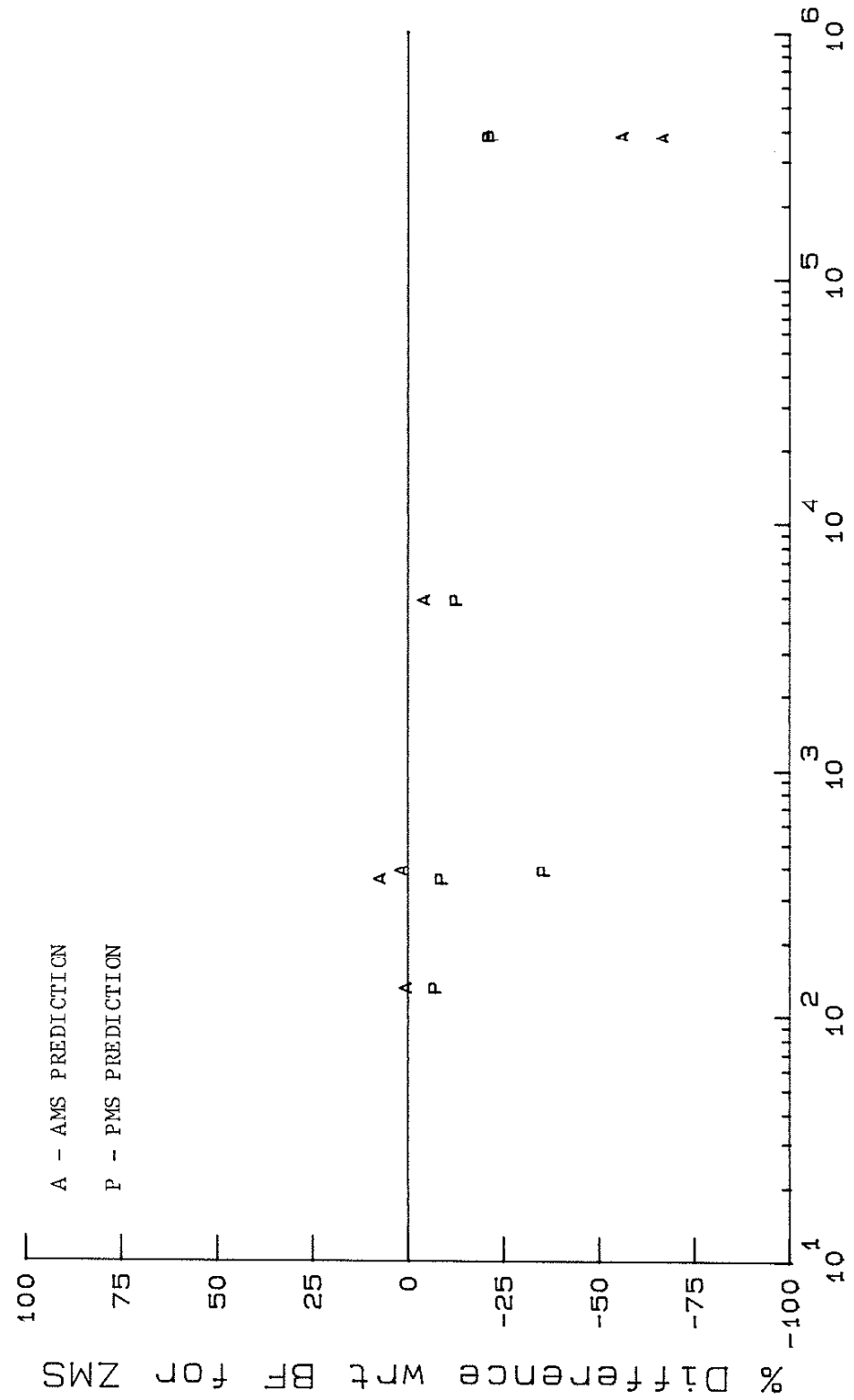

FIG. 25 COMPARISON OF MEAN STRESS PREDICTION METHODS, HISTORY AX

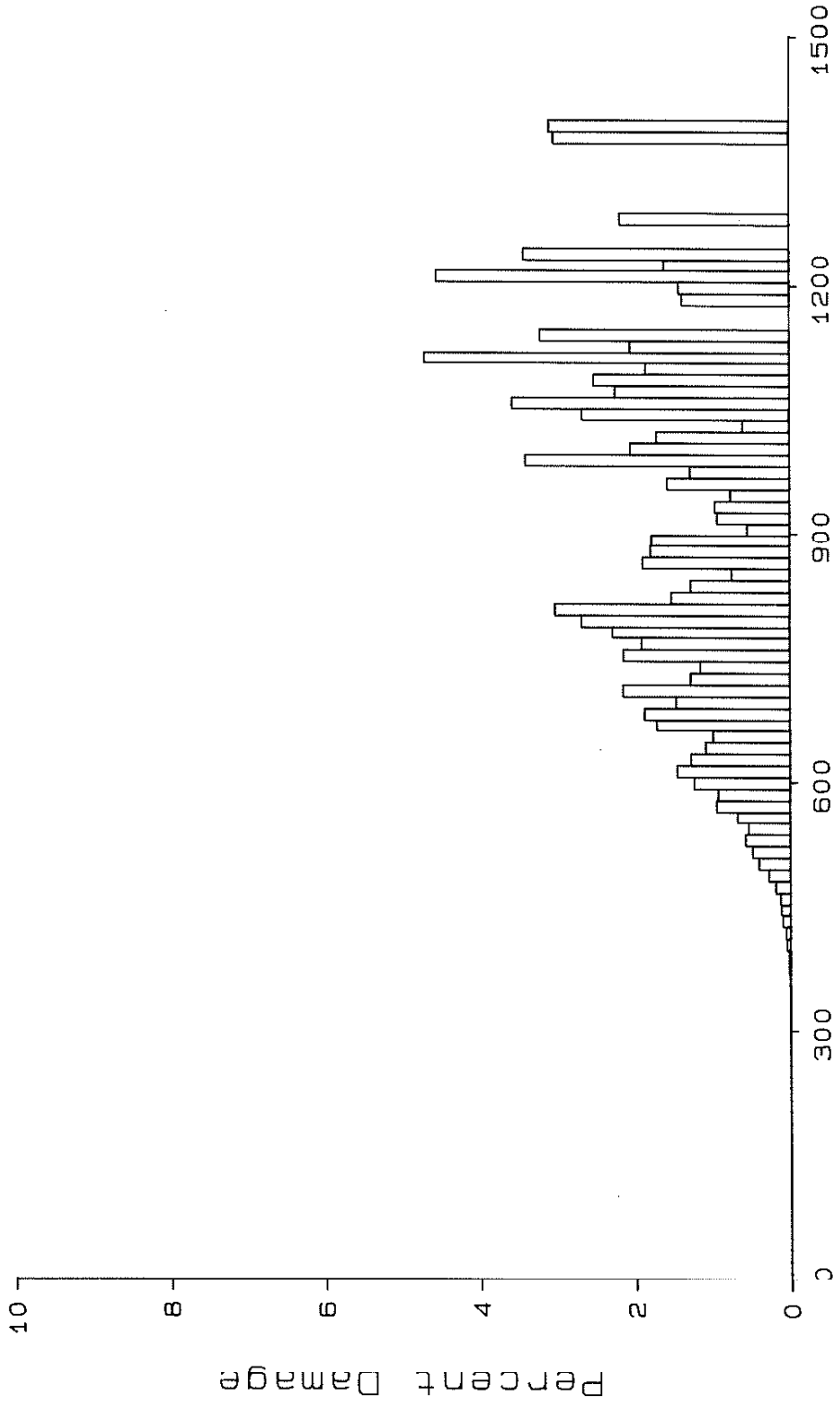

FIG. 26 DAMAGE DISTRIBUTION FOR STRAIN HISTORY A

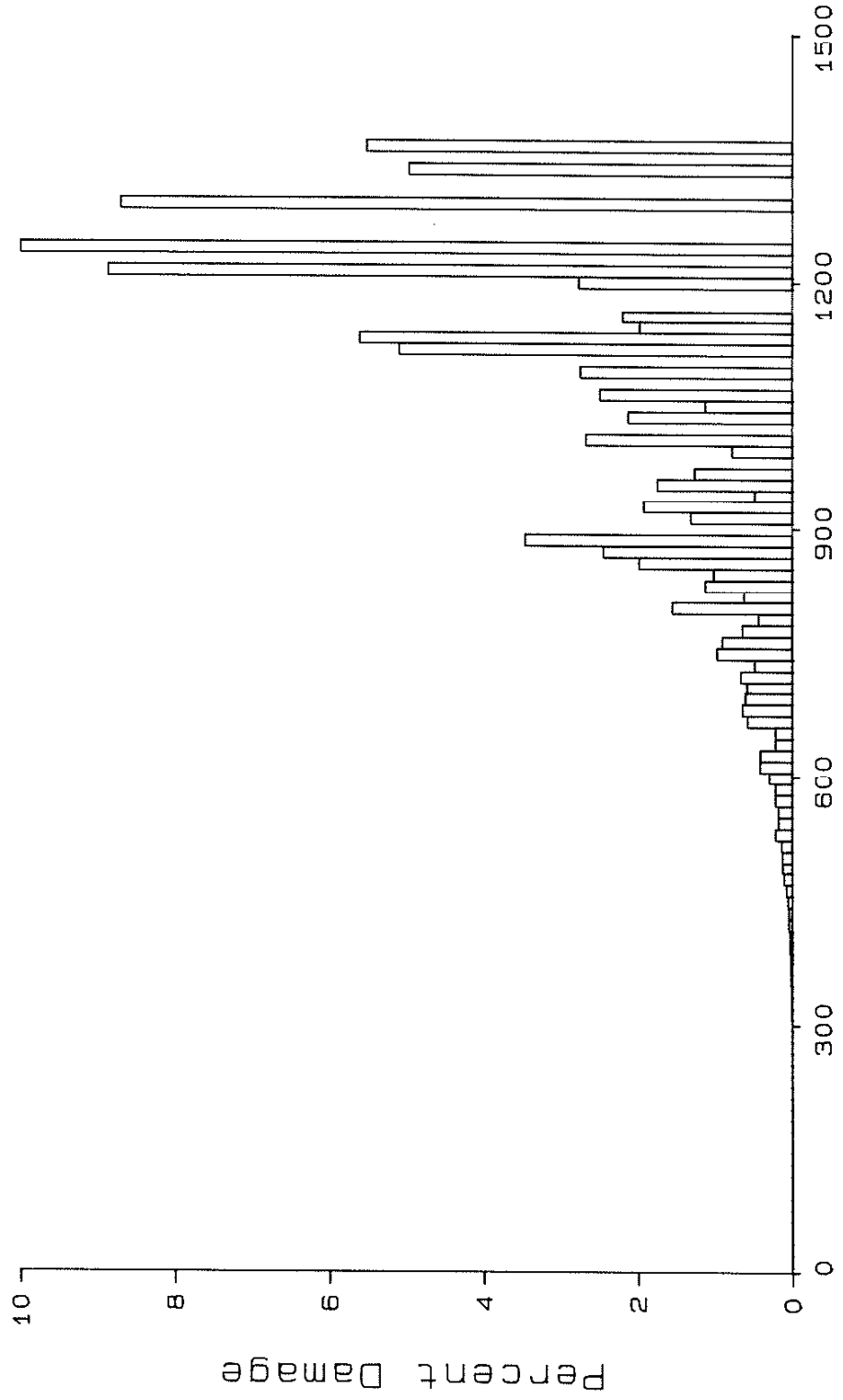

FIG. 27 DAMAGE DISTRIBUTION FOR STRAIN HISTORY B

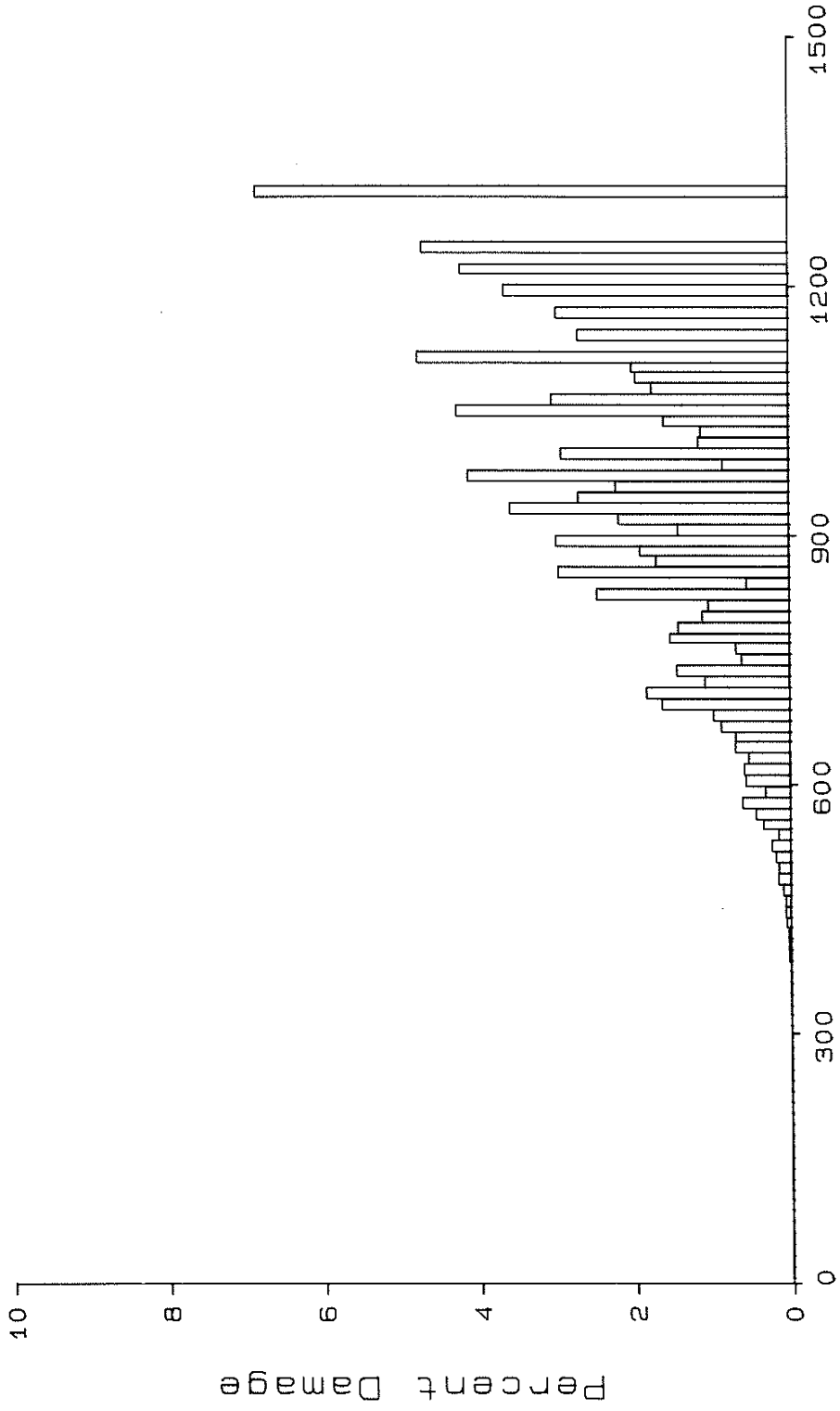

FIG. 28 DAMAGE DISTRIBUTION FOR STRAIN HISTORY C

REFERENCES

[1] Wetzel, R. M., Ed., Fatigue under Complex Loading: Analysis and Experiments, Advances in Engineering, Vol. 6, Society of Automotive Engineers, Warrendale, Pa., 1977, 207 pp.

[2] Landgraf, R. W., "Fundamentals of Fatigue Analysis," Proceedings of the SAE Fatigue Conference P-109, April 14-16, 1982, pp. 11-16.

[3] Manson, S. S., "Behavior of Materials under Conditions of Thermal Stresses," Heat Transfer Symposium, University of Michigan Engineering Research Institute, 1953, pp. 9-75.

[4] Coffin, L. F., Jr., "A Study of Cyclic Thermal Stresses on a Ductile Metal," Transactions ASME, Vol. 76, 1954, pp. 931-950.

[5] Martin, J. F., "Computer Based Simulation of Cyclic Stress-Strain Behavior," M.S. Thesis, Department of Theoretical and Applied Mechanics, University of Illinois, Urbana, Ill., 1969.

[6] Wetzel, R. M., "A Method of Fatigue Damage Analysis," Ph.D. Thesis, Department of Civil Engineering, University of Waterloo, Ontario, Canada, 1971.

[7] Dowling, N. E., "Fatigue Failure Predictions for Complicated Stress-Strain Histories," Journal of Materials, Vol. 7, No. 1, March, 1972, pp. 71-87.

[8] Socie, D. F. and P. Kurath, "Cycle Counting for Variable Amplitude Crack Growth," Fracture Mechanics: Fourteenth Symposium - Vol. II: Testing and Applications, J. C. Lewis and G. Sines, Editors, American Society for Testing and Materials, 1983, pp. II-19 - II-32.

[9] Miner, M. A., "Cumulative Damage in Fatigue," Journal of Applied Mechanics, Transactions ASME, Vol. 12, September, 1945, pp. A159-A164.

[10] Leve, H. L., "Cumulative Damage Theories," Metal Fatigue: Theory and Design, A. F. Madayag, Ed., John Wiley and Sons, Inc., 1969, pp. 171-203.

[11] "Mechanical Testing of Steel Products, A370-77," 1983 Annual Book of ASTM Standards, Section 3, Metals Test Methods and Analytical Procedures, American Society of Testing and Materials, 1983, pp. 1-7.

[12] Landgraf, R. W., JoDean Morrow and T. Endo, "Determination of the Cyclic Stress-Strain Curve," Journal of Materials, Vol. 4, No. 1, 1969, pp. 176-188.

[13] "Standard Definitions of Terms Relating to Constant Amplitude, Low Cycle Fatigue Testing E606-80," 1983 Annual Book of ASTM Standards, Section 3, Metals Test Methods and Analytical Procedures, American Society of Testing and Materials, 1983, pp. 652-669.

[14] Raske, D. T. and JoDean Morrow, "Mechanics of Materials in Low Cycle Fatigue Testing," Manual on Low Cycle Fatigue Testing, ASTM STP 465, American Society for Testing and Materials, 1969, pp. 1-25.

[15] Morrow, JoDean, "An Analysis of Cyclic Stress-Strain Behavior for Conditions of Controlled Strain," Ph.D. Thesis, Department of Theoretical and Applied Mechanics, University of Illinois, Urbana, Ill., 1957.

[16] Morrow, JoDean and D. F. Socie, "The Evolution of Fatigue Crack Initiation Life Prediction Methods," Experimentation and Design in Fatigue, Proceedings of Fatigue 1981, F. Sherratt and J. B. Sturgeon, Eds., Society of Environmental Engineers, Warwick University, England, Westbury House, 1981, pp. 1-21.

[17] Dowling, N. E., "Fatigue Failure Predictions for Complicated Stress-Strain Histories," Journal of Materials, Vol. 7, No. 1, March, 1972, pp. 71-87.

[18] Downing, S. D. and D. F. Socie, "Simple Rainflow Counting Algorithms," International Journal of Fatigue, Vol. 4, No. 1, 1982, pp. 31-40.

[19] Manson, S. S. and G. R. Halford, "Practical Implementation of the Double Linear Damage Rule and Damage Curve Approach for Treating Cumulative Fatigue Damage," NASA Technical Memorandum 81517, NASA Lewis Research Center, Cleveland, Ohio, April, 1980, 49 pp.

[20] Corten, H. T. and T. J. Dolan, "Cumulative Fatigue Damage," Proceedings of the International Conference on Fatigue of Metals, London, Institution of Mechanical Engineers and American Society of Mechanics Engineers, 1956, pp. 235-246.

[21] Socie, D. F. and P. J. Artwohl, "Effect of Spectrum Editing on Fatigue Crack Initiation and Propagation in a Notched Member," Fracture Control Program Report No. 31, University of Illinois, College of Engineering, Urbana, Ill., December, 1978, 17 pp.

[22] Dieter, G. E., Jr., Mechanical Metallurgy, McGraw-Hill, Second Edition, 1976, pp. 344-346.